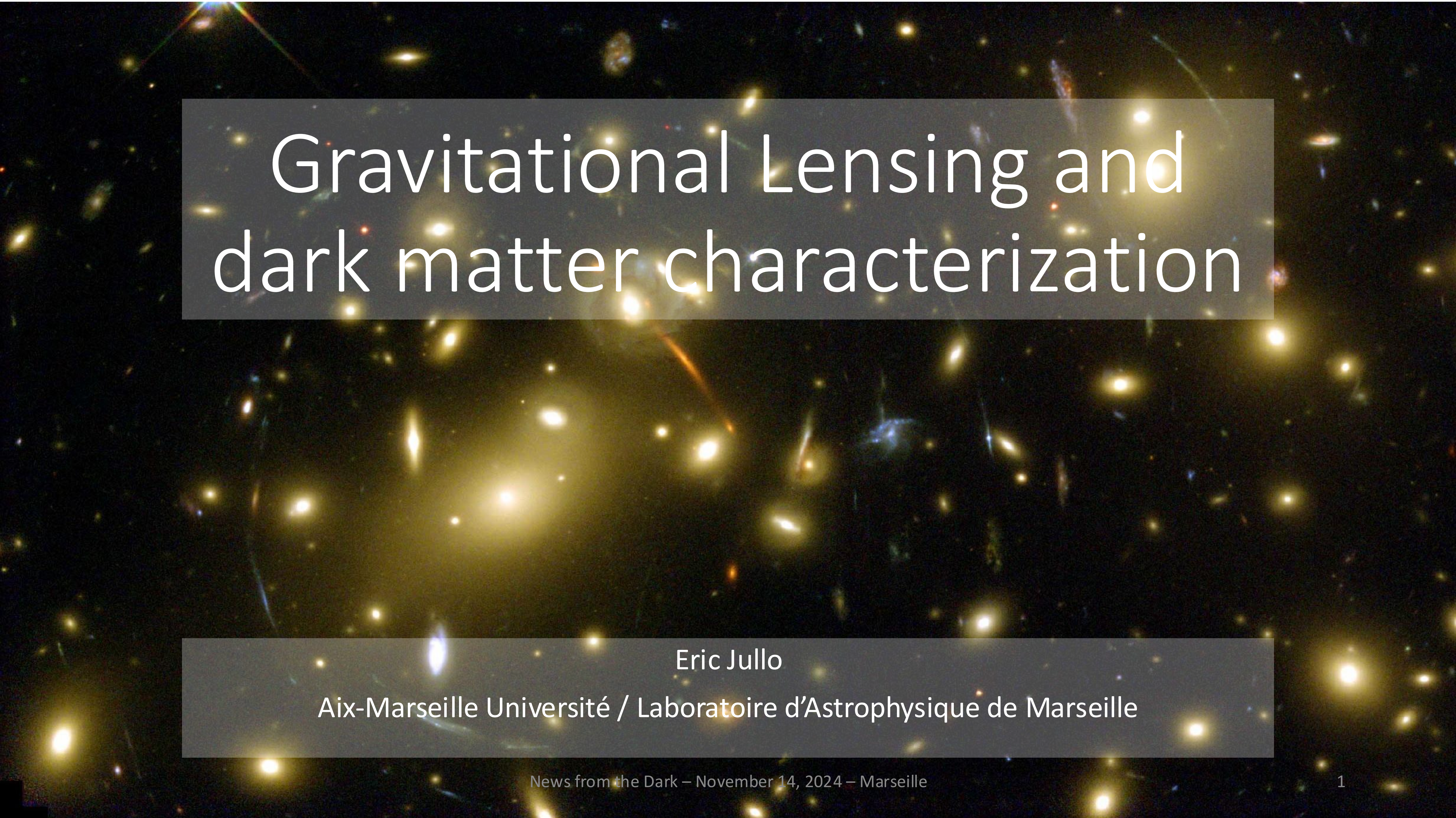

Gravitational Lensing and dark matter characterization

Eric Jullo

Aix-Marseille Université / Laboratoire d'Astrophysique de Marseille

James Webb Space Telescope (JWST) vs Hubble

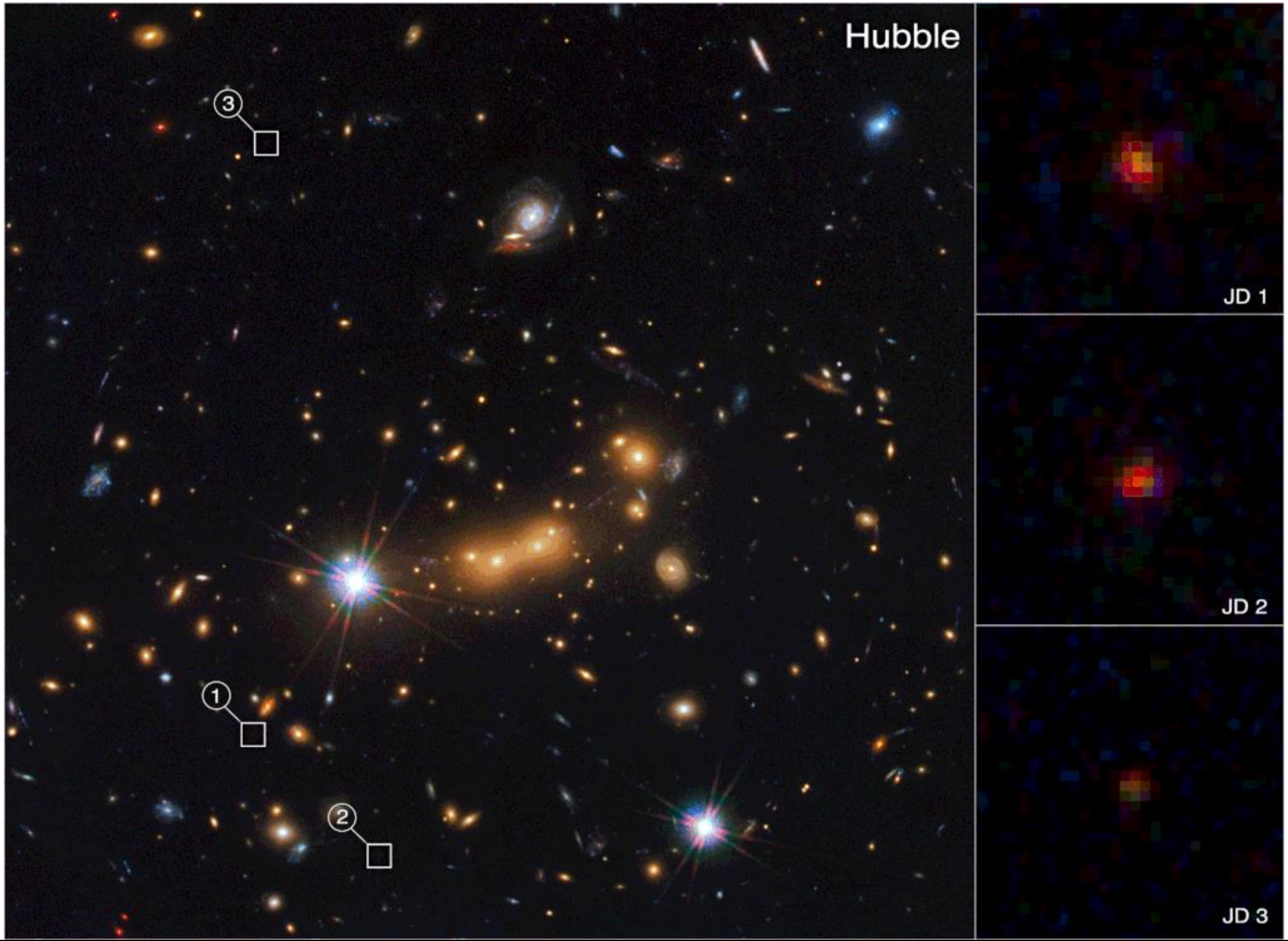

https://www.spaceze.com/news/jwst-sees-the-same-galaxy-from-three-different-angles-thanks-to-a-gravitational-lens

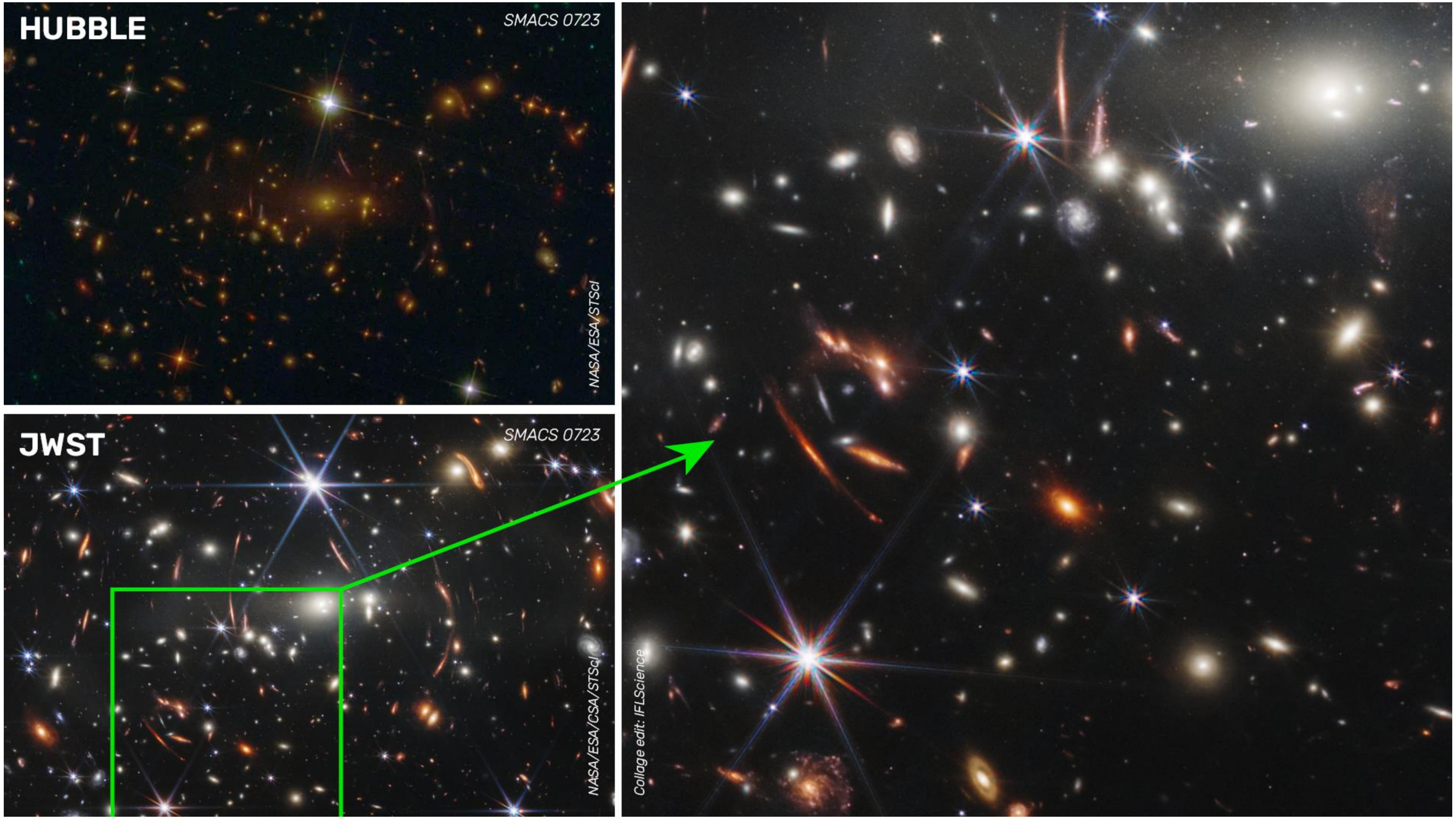

https://www.iflscience.com/what-are-we-actually-seeing-in-jwsts-first-deep-field-image-64410

Dark Matter direct detection sensitivities

Experiments / prototypes in preparation at CPPM:

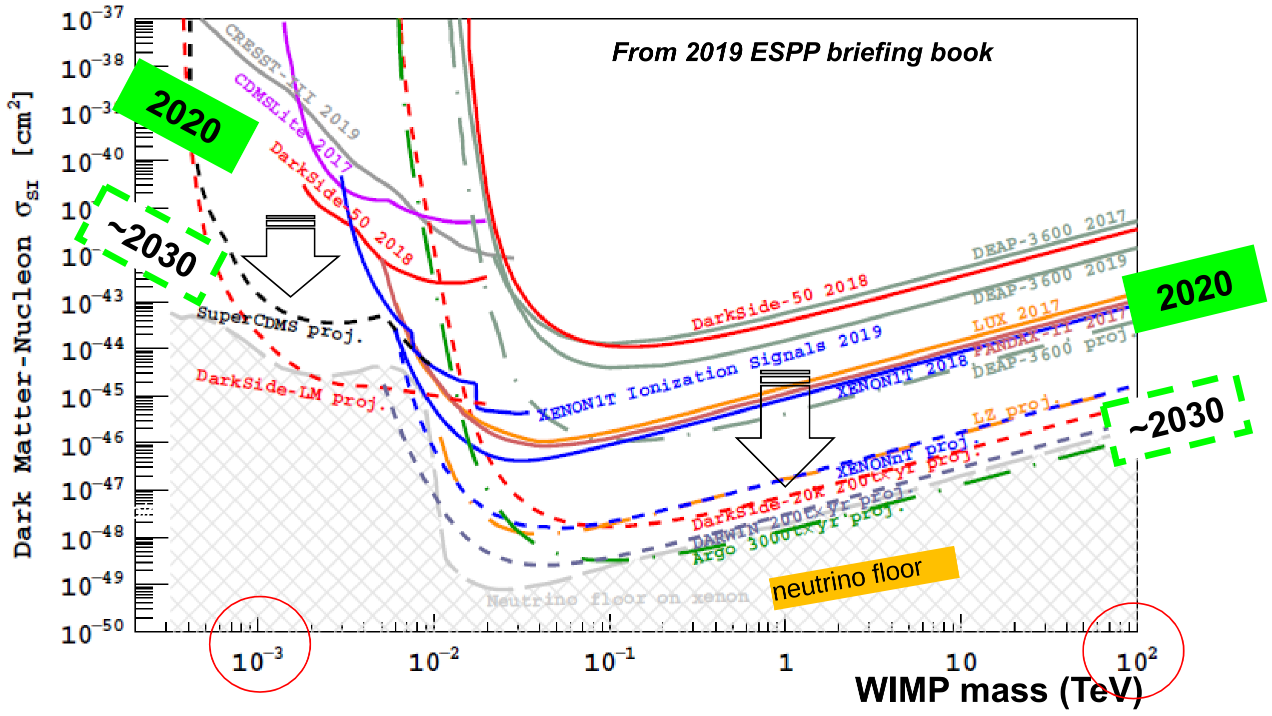

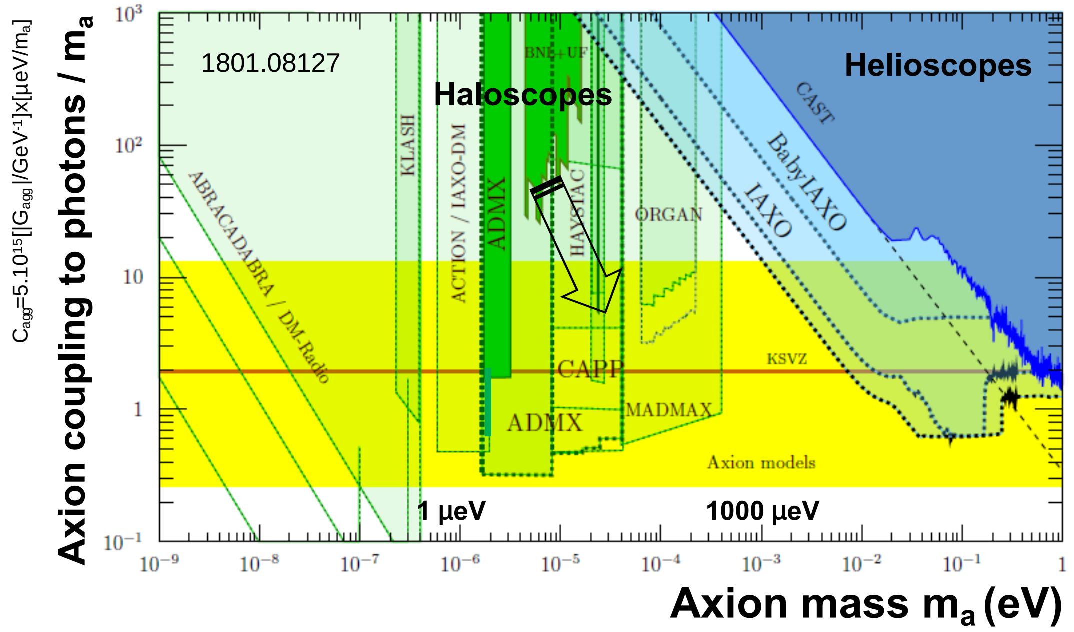

DarkSide-20k

➔TPC with noble liquid (Xe, Ar): best limits 1 GeV - 100 TeV

➔Next decade decisive to probe WIMPs down to neutrino floor

MADMAX

➔ Targets “high mass” DM axions: **m_a~40-400 µev**

➔ R&D program to improve signal sensitivity

Dark matter in large scale structure context

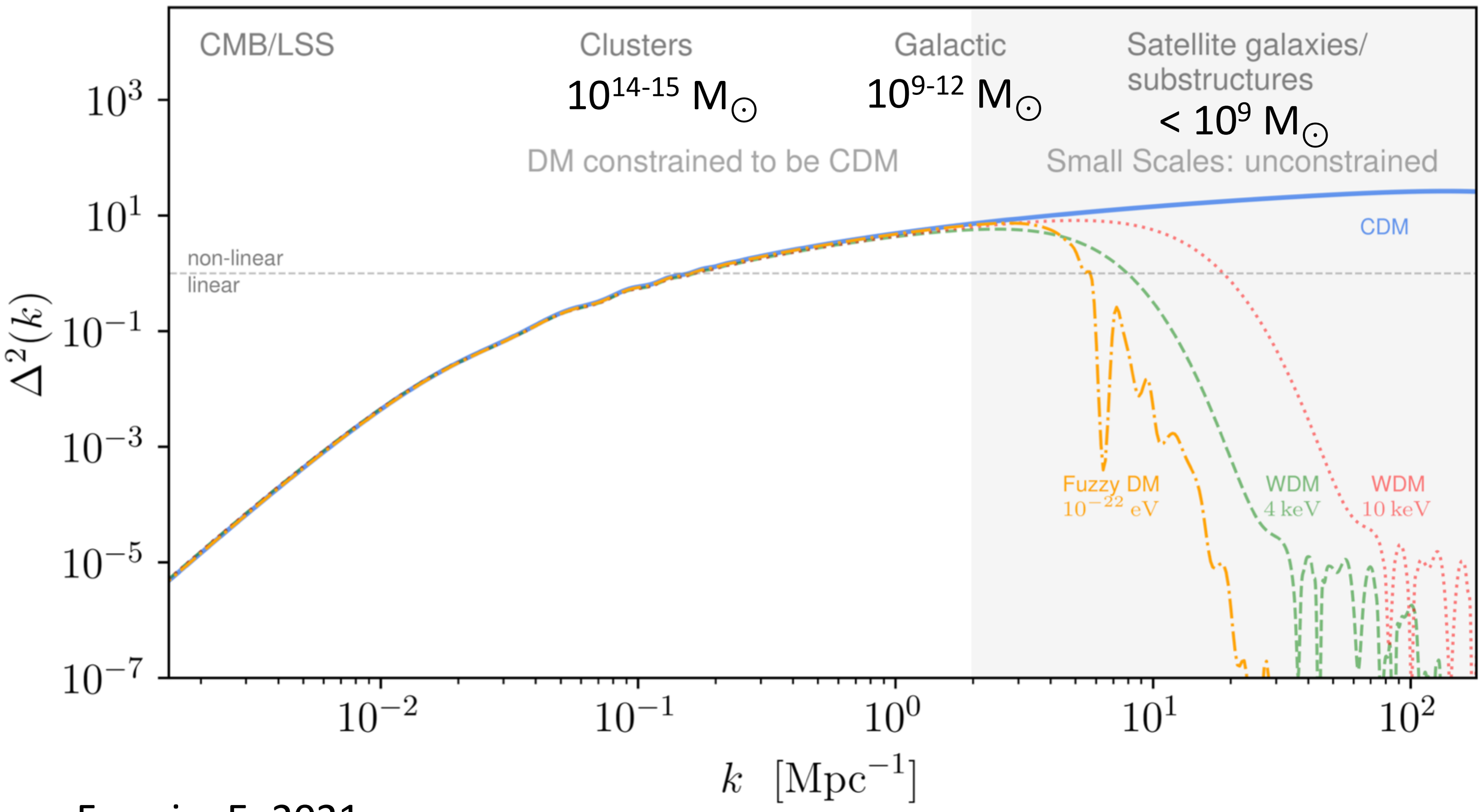

Ferreira E. 2021

Cold vs Warm dark matter observables

Mass-Concentration relation

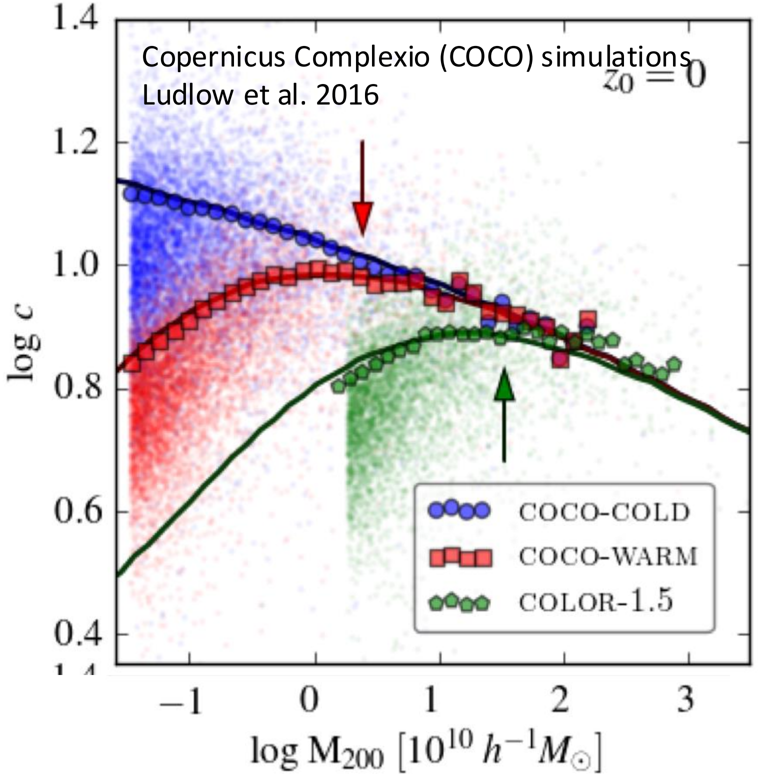

Halo mass function

Sownak et al. 2015

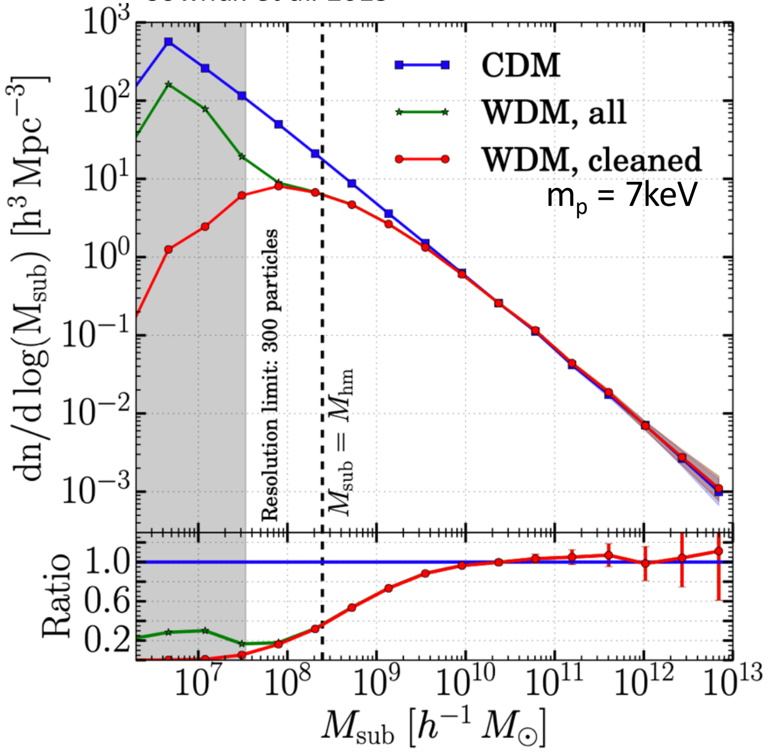

Sub-Halo mass function

Snowak et al. 2017

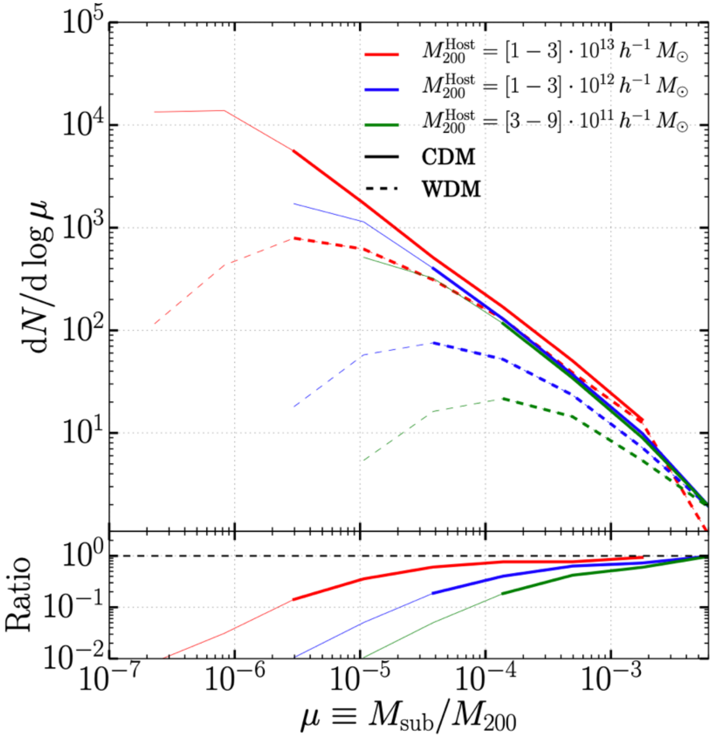

Galaxy cluster profile in SIDM

Robertson et al. 2019

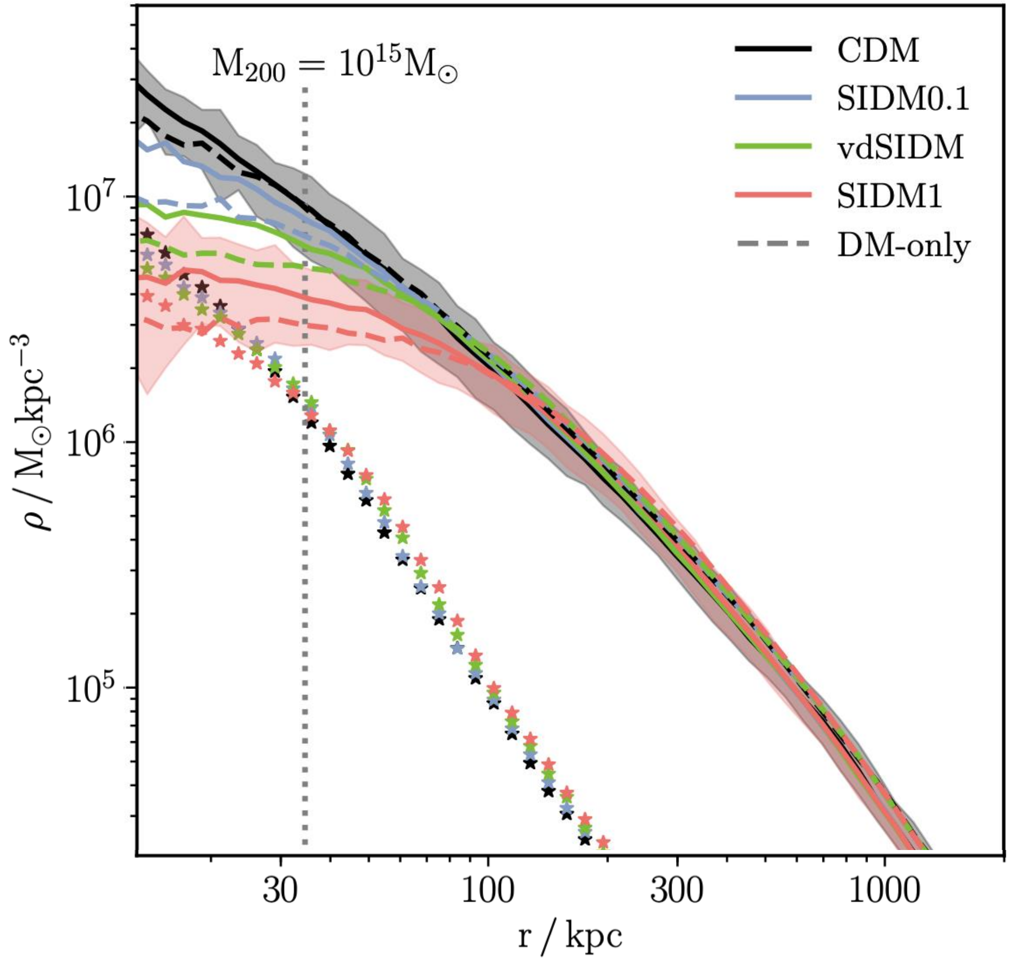

Kaplinghat et al. 2016

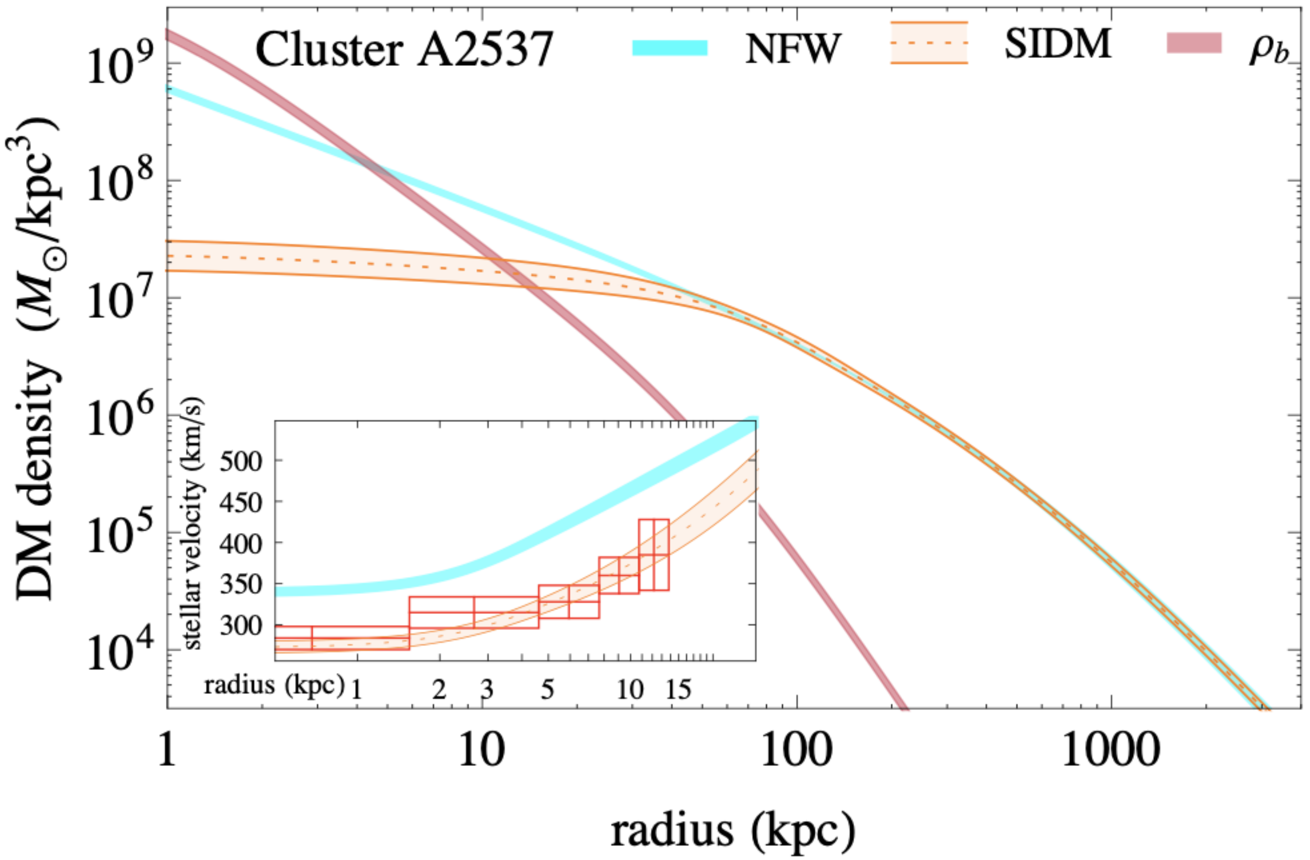

In simulations, dark matter can partially be distinguished from baryons at scales R < 20 kpc

The central density profile slope of ETG

Bolton et al. 2008

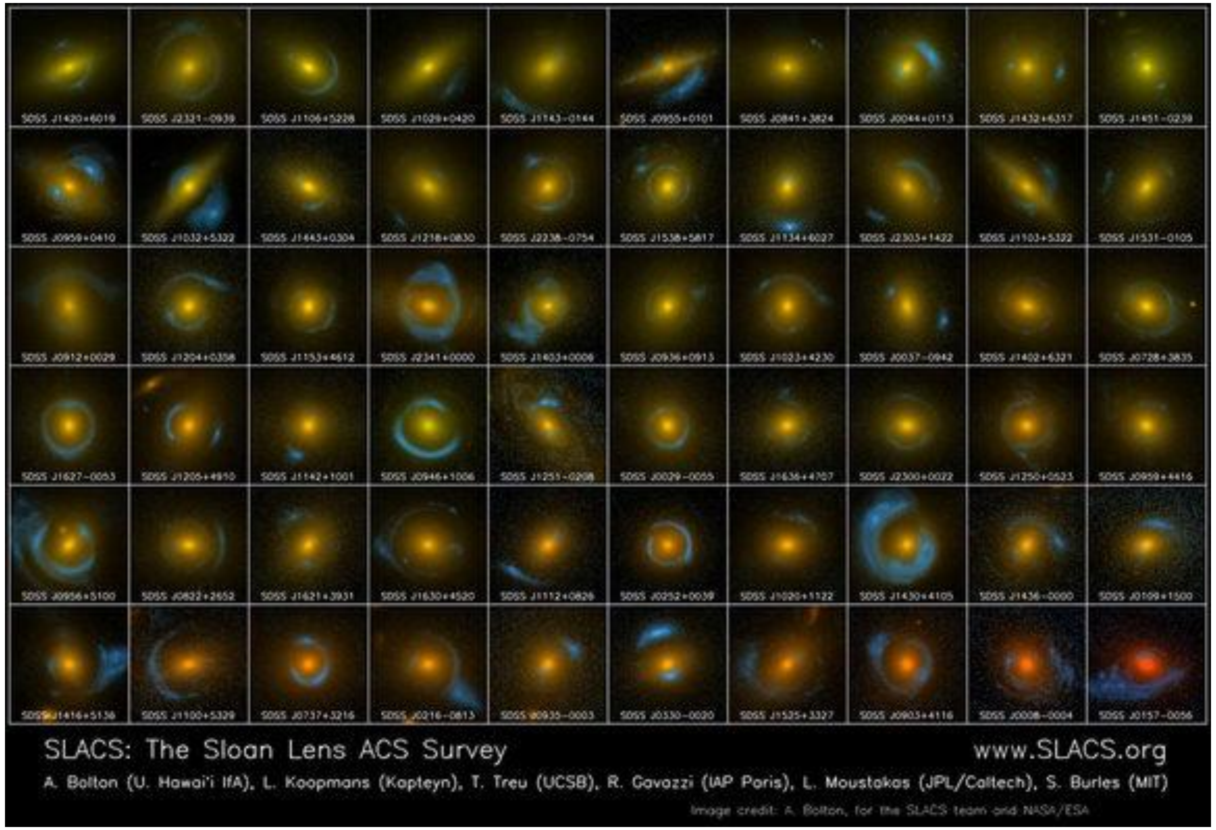

SLACS: 58 elliptical galaxies with gravitational arcs detected in SDSS spectra

Combination of SL mass in Einstein radius, and velocity dispersion of the stars σ_0 in SDSS spectra (R_{fiber} = 3")

Confirmation that Early Type Galaxies (ETG) follow isothermal density profile γ = 2 **on average**

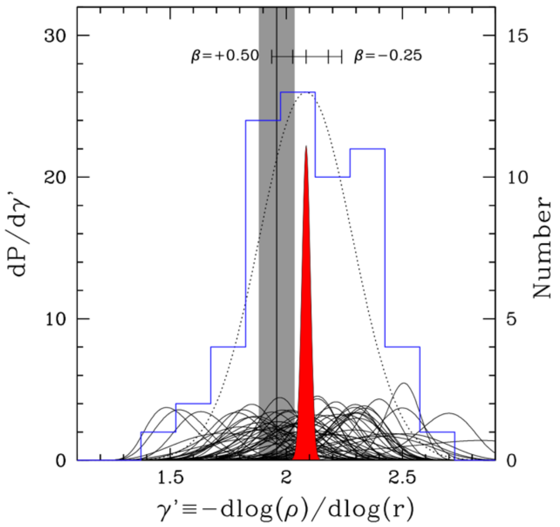

Koopmans et al. 2009

The Strong Lensing Legacy Survey (SL2S)

Combination of 25 lenses from SL2S, 53 from SLACS and 4 from Lenses Structure and Dynamics (LSD)

- Redshift range : $0.2 < z < 0.8$
- Stellar mass range: $\log M^* / M_\odot = 11 - 12$
- Galaxy size range: $R_{eff} = 1 - 20$ kpc

=> Understand the DM profile slope γ' variation

$$\frac{\partial \gamma'}{\partial z} = \alpha = -0.31 \pm 0.10,$$

$$\partial \gamma' / \partial \log \Sigma_* = 0.38 \pm 0.07$$

Sonnenfeld et al. 2013

Cabanac et al. 2007, Gavazzi et al. 2012

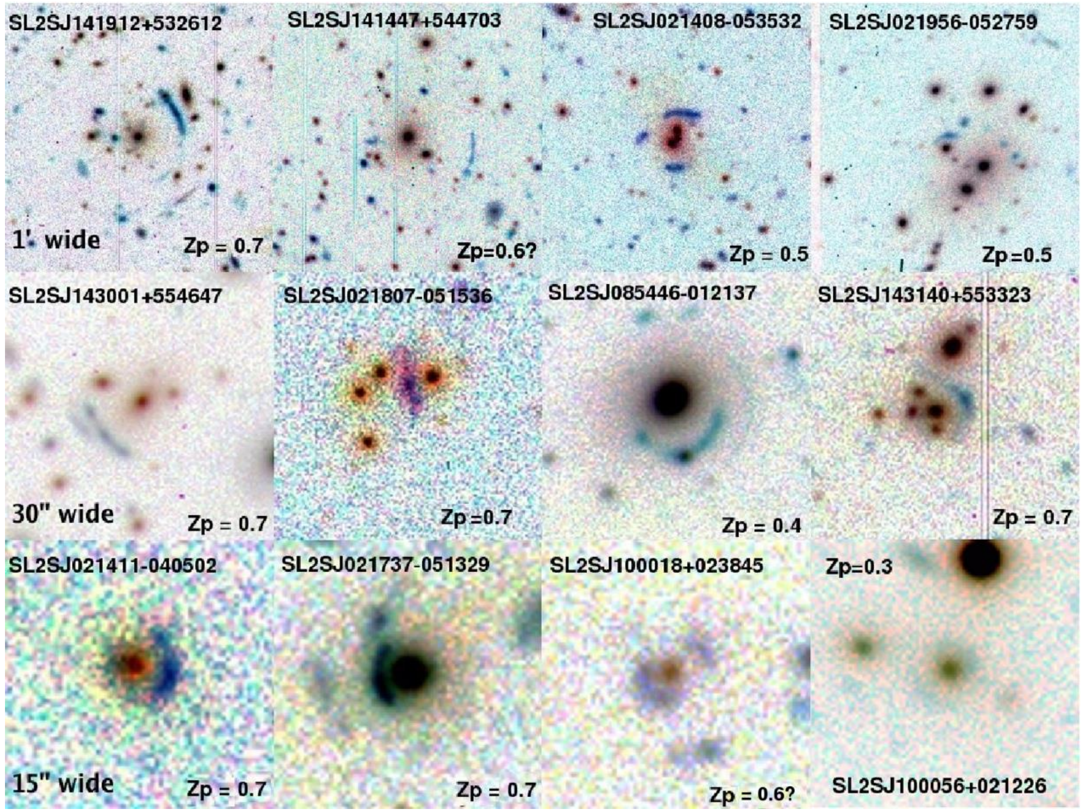

=> The slope is rather constant $\langle\gamma'\rangle = 2$, but this hides degeneracies:

- Stellar mass increases on the edges
- DM infall in the center (+contraction)

} Slope γ' unchanged

Same results found in Li, Shu & Wang 2018

Stellar Initial Mass Function with MANGA

Li, Ge, Mao et al. 2017

MANGA observed in IFU mode 17 galaxies on $7deg^2$ of sky (1423 fibers total, Bundy et al. 2015)

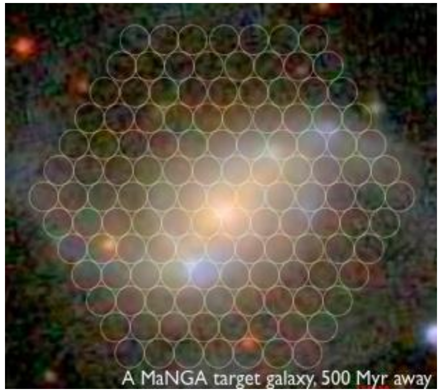

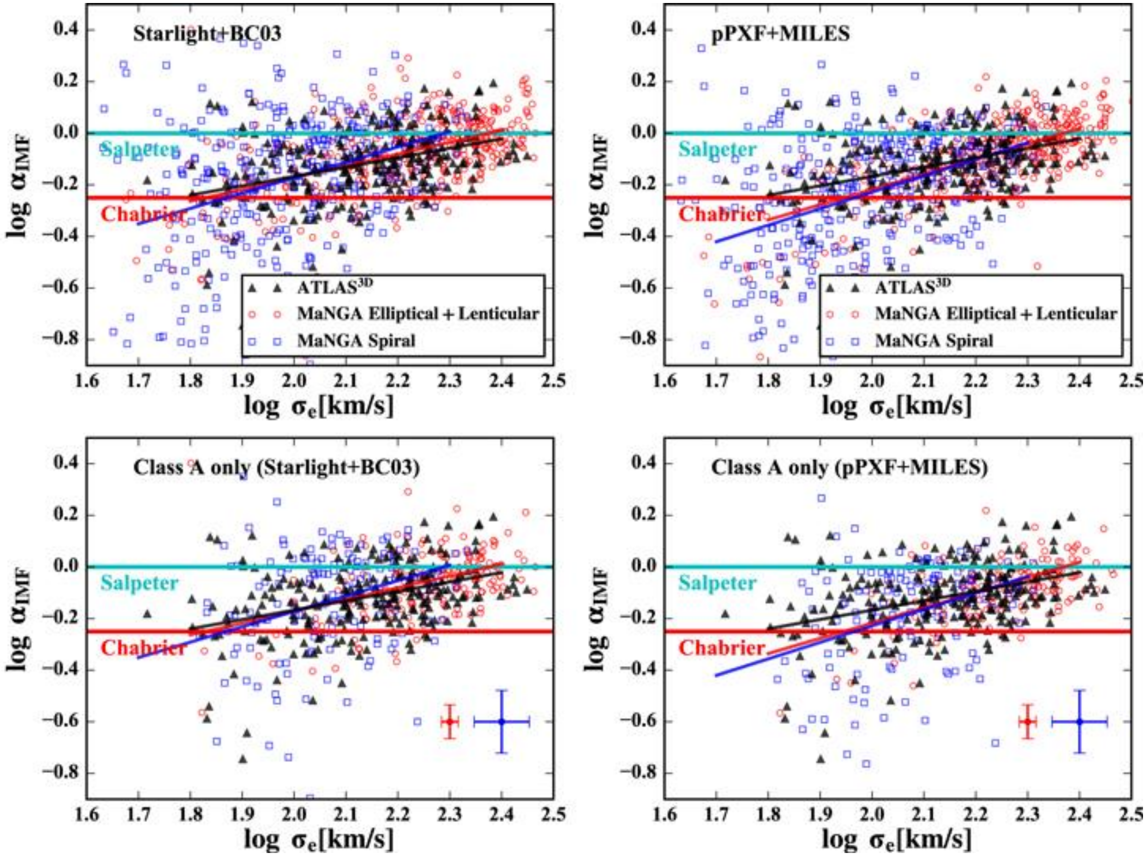

Measurement of IMF mismatch

$$\alpha_{\rm IMF} \equiv (M^*/L)^{\rm nogas}_{\rm JAM} / (M^*/L)_{\rm SPS}$$

=> α_{IMF} increases with σ_e (±50% uncertainty)

Strong-lensing, dynamics & weak-lensing

7 galaxy clusters selected w/ SL arcs

Newman et al. 2014

DM density profile gNFW: free inner slope γ to account for adiabatic contraction

Stellar mass M* derived from Stellar Population Synthesis => IMF assumption (quoted factor ~2 uncertainty)

Stellar density profile adjusted to Surface Brightness of central BCG, and scaled to $\alpha_{SPS} \times M^*$

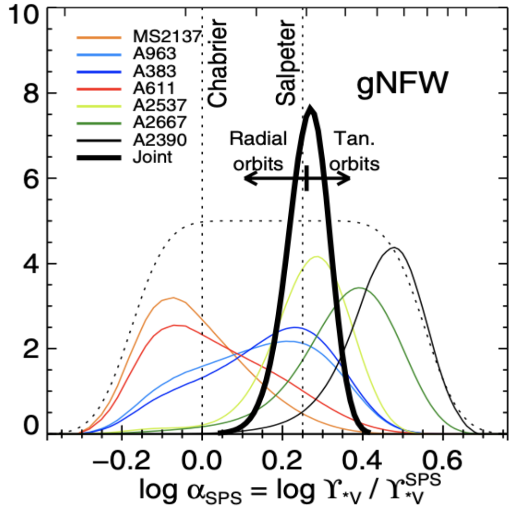

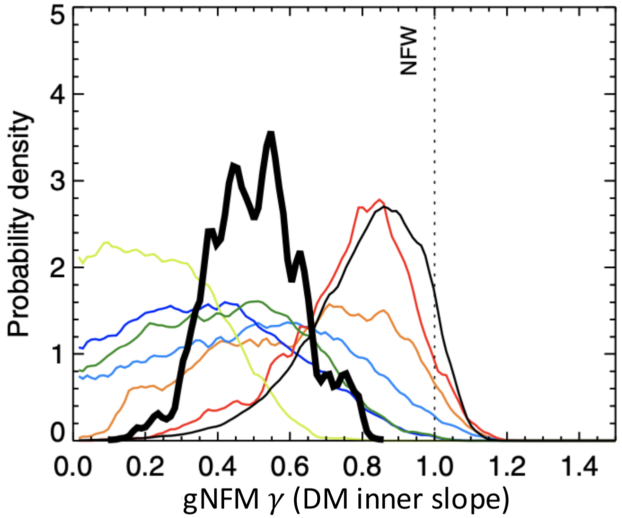

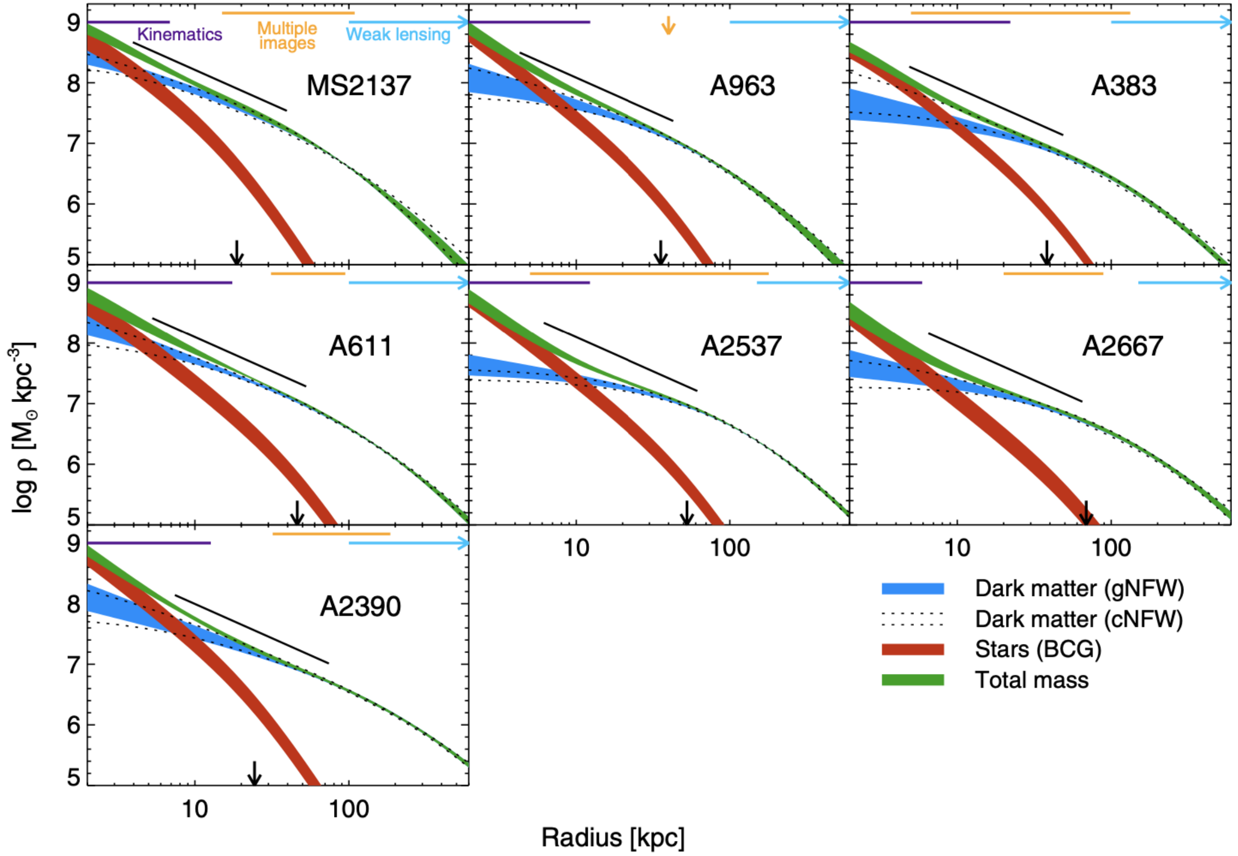

=> Galaxy clusters have a flat cored DM profile γ = 0.5±0.13

Averaging over more clusters and groups

Wang C., Li R. et al. 2024

Weak Lensing for the larger scales and stellar kinematics in the center with MANGA (IFU) data

Stellar density profile adjusted on r-band SB distribution scaled to α_{SPS} × M*

=> The DM profile inner slope is $\gamma > 1$

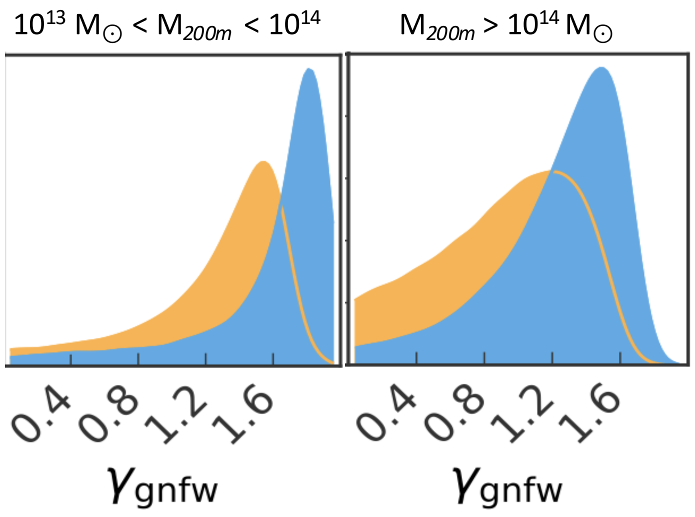

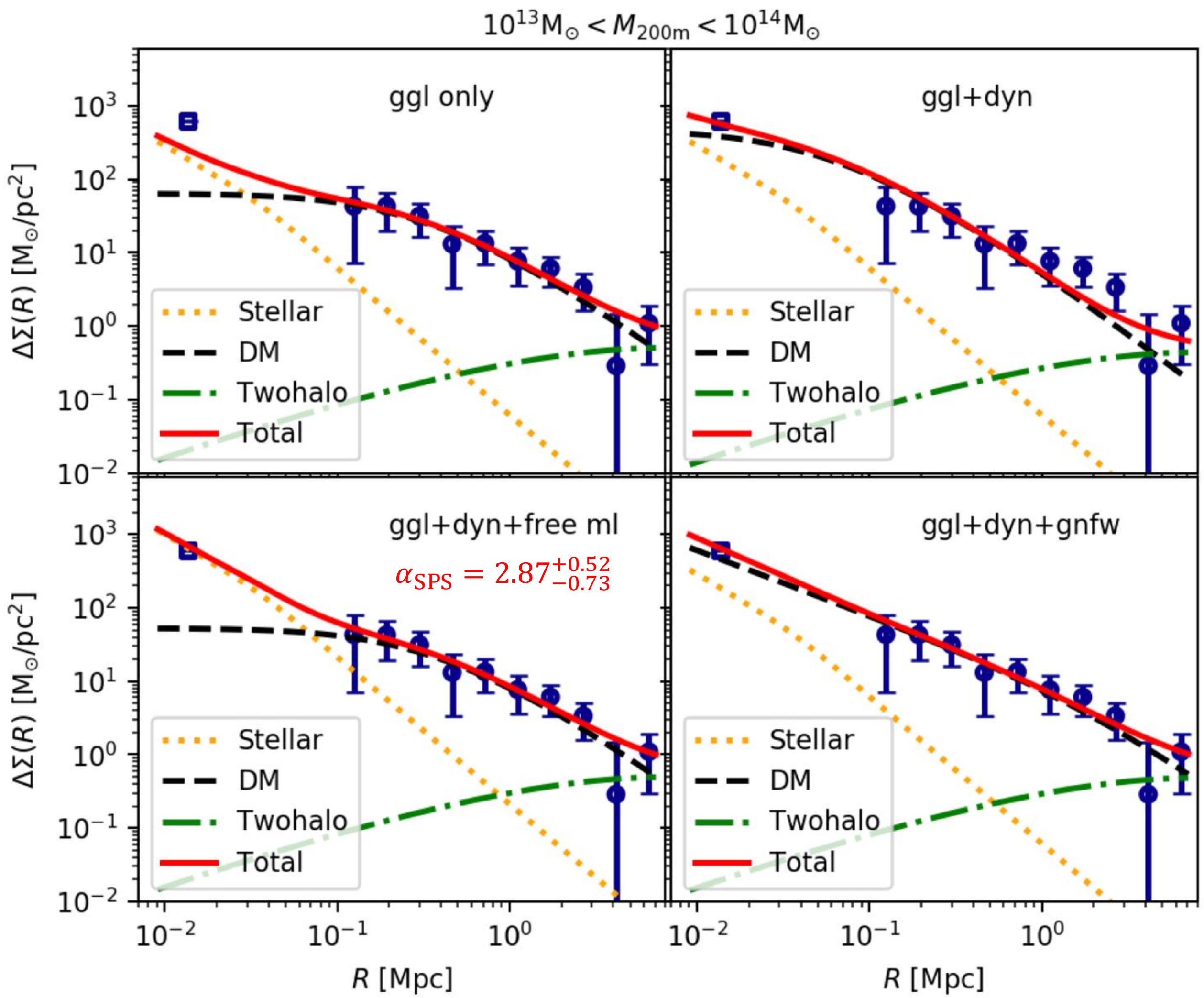

Strong lensing in galaxy clusters

Better modelling thanks to
- More multiple images constraints with deep HST observations (HFF program, JWST)
- Integral field spectroscopy data to constrain galaxy kinematics (MUSE)
- Dark matter and stellar content decoupled from the cluster DM component

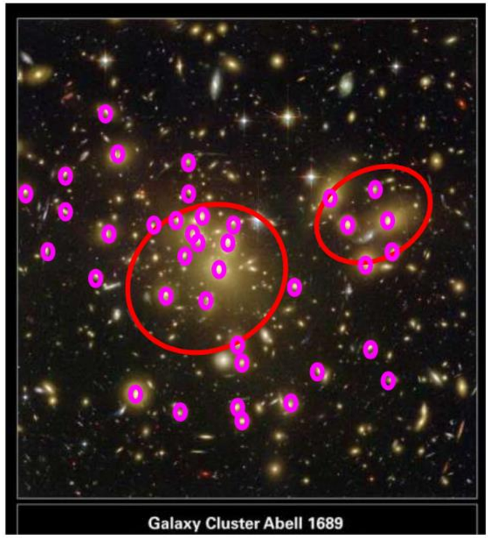

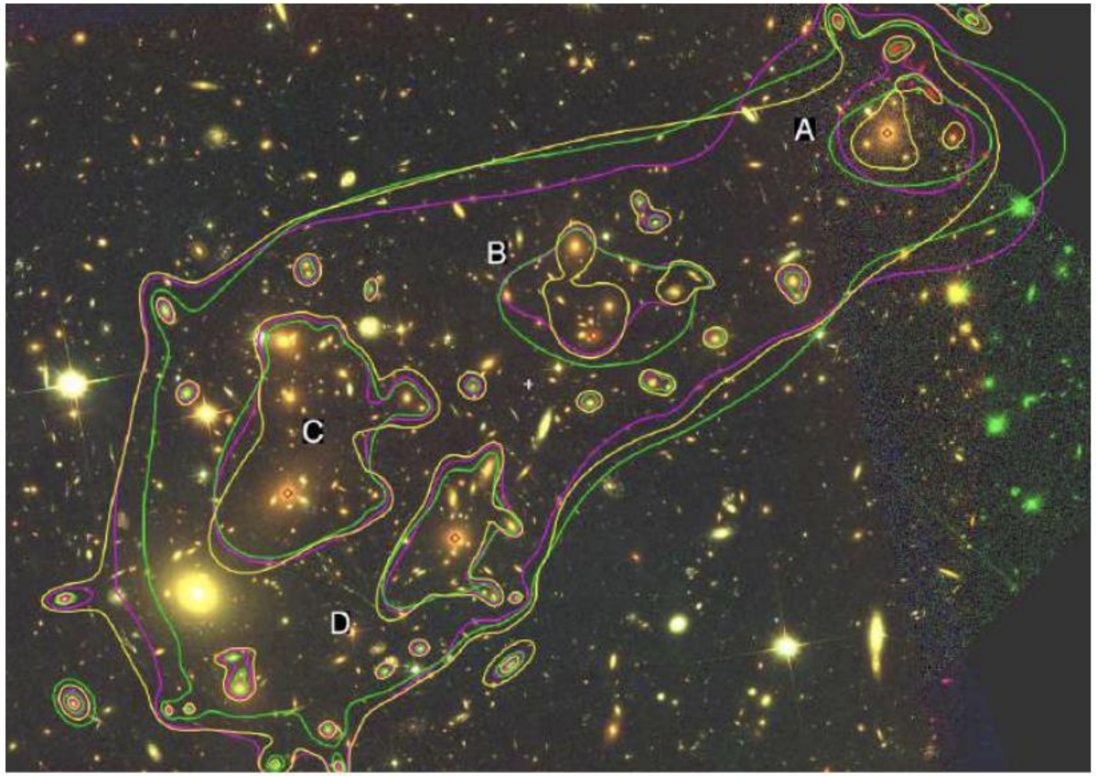

Limousin et al. 2017

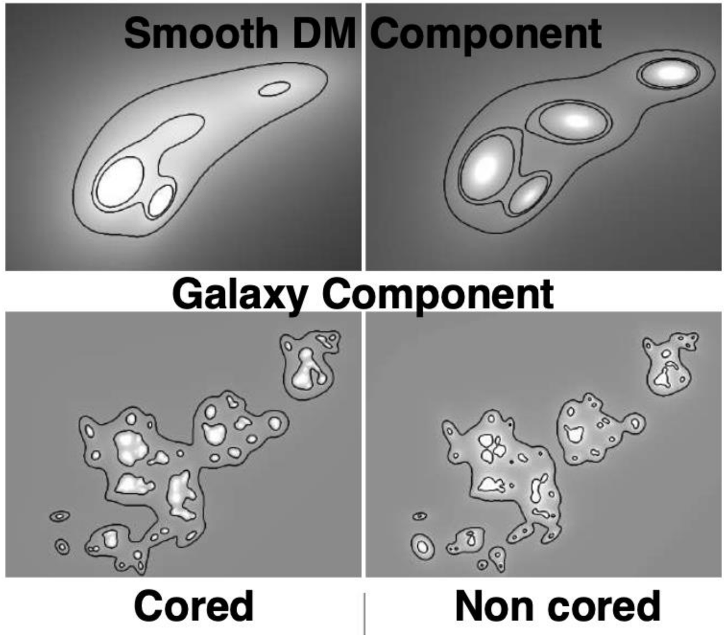

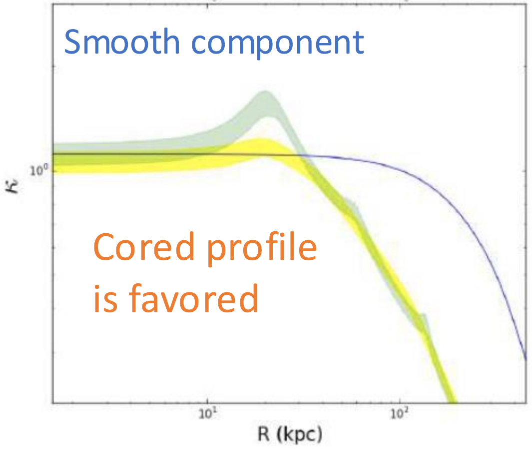

Limousin et al. 2022

=> Hint for self-Interacting DM? Or systematic bias? => need bigger sample

Sub-Structures in galaxy clusters

- Light 2.5keV WDM (red curve) => few subhalos overall

- σ/m = 1.0 cm^2/g SIDM (dark green) => low counts at small radius

  => Heat transfert between 'hot' host DM, and 'cool' subhalo DM

  => Enhanced tidal stripping (disruption) because of cored density profile of subhaloes

- f(R) cosmology could also impact the mass segregation function (Arnolds & Li, 2019), because f(R)-gravity increases the number of low-mass halos (not screened)

Stafford et al. 2019

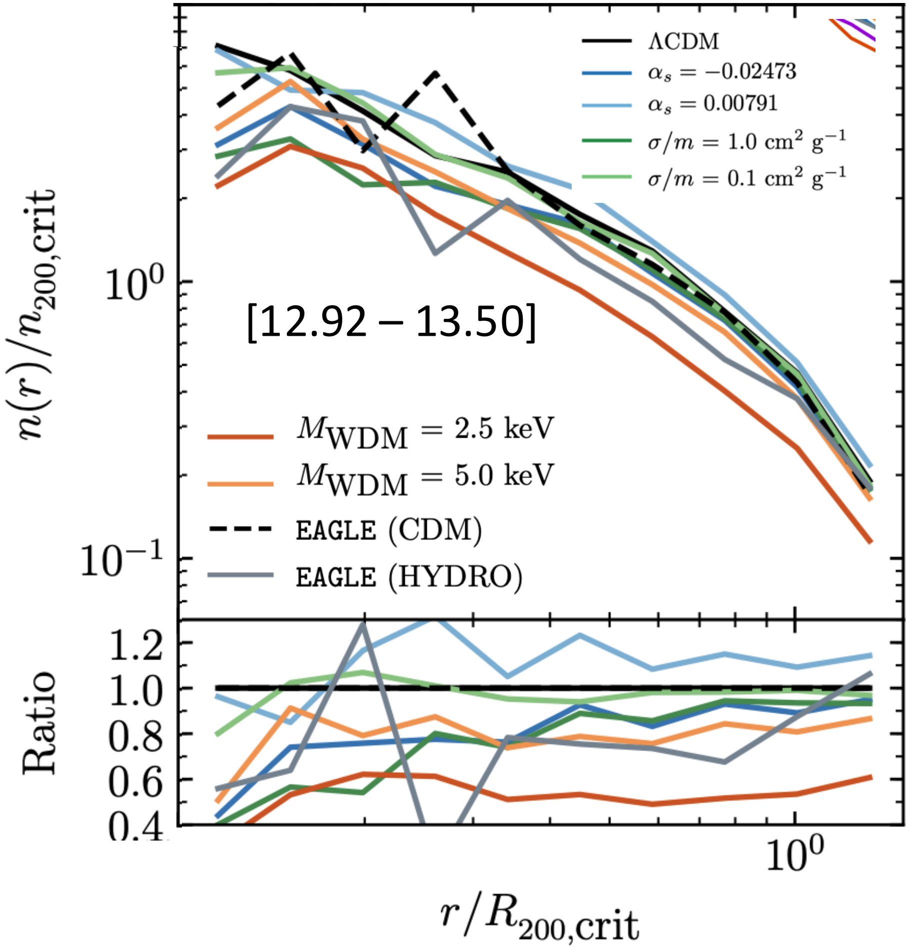

Tidal stripping in galaxy clusters

- Modeling of DM distribution with SL constraints
- Comparison of subhalo mass function & radial distribution with hydro-simulations
- Subhalo disruption due to tidal stripping in simulations

=> need more compact cores (stars?)

Natarajan et al. 2017

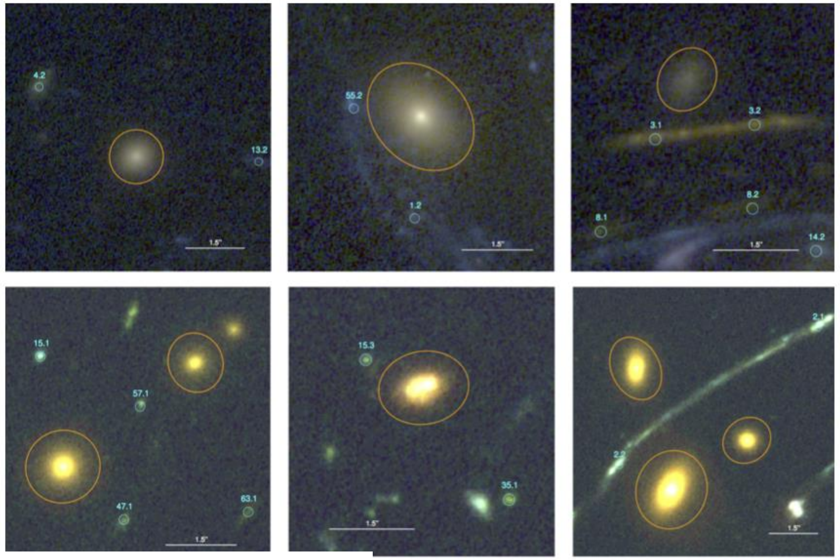

subhalo mass function

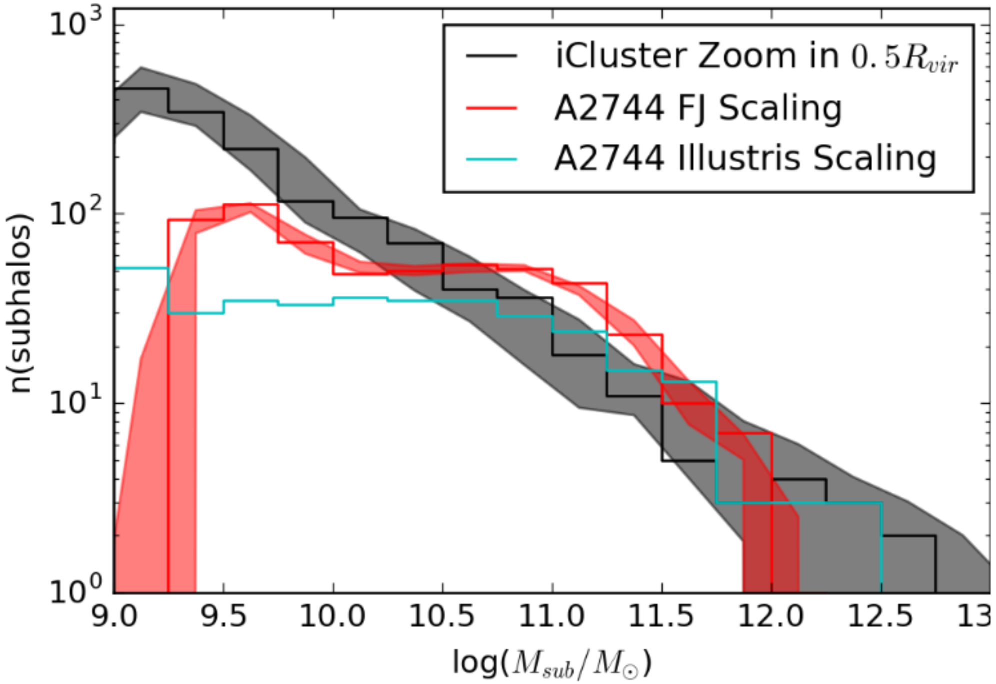

Radial distribution

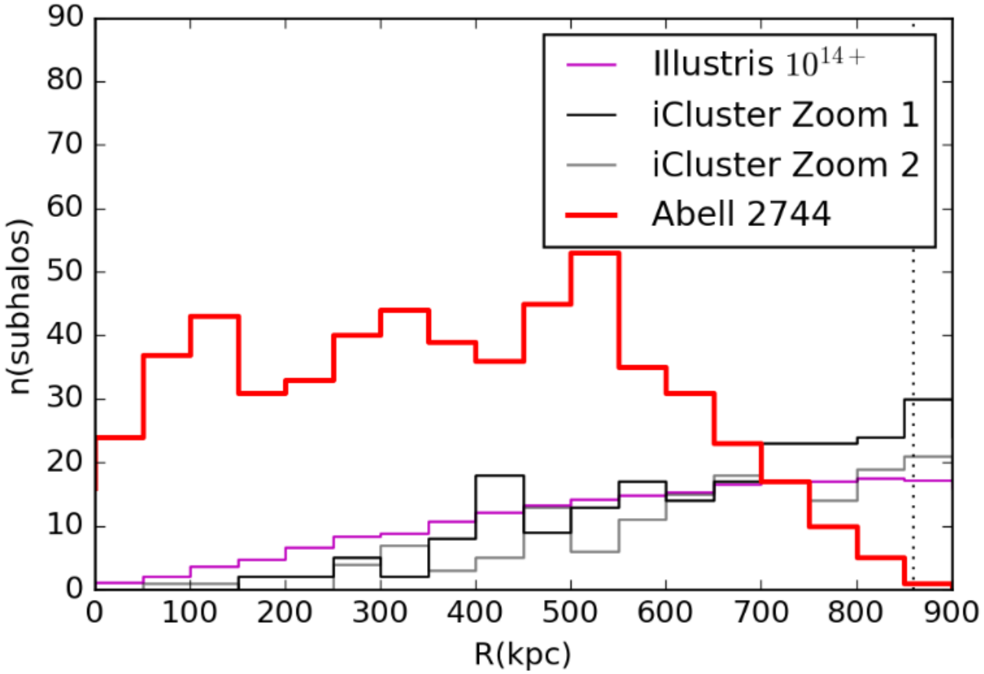

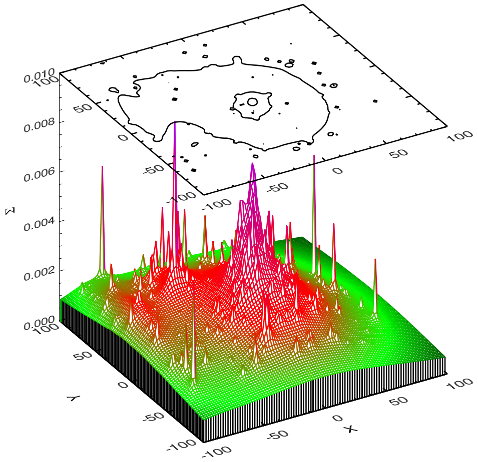

Sub-structures traced by GGSL in galaxy clusters

Meneghetti et al. 2020, 2022

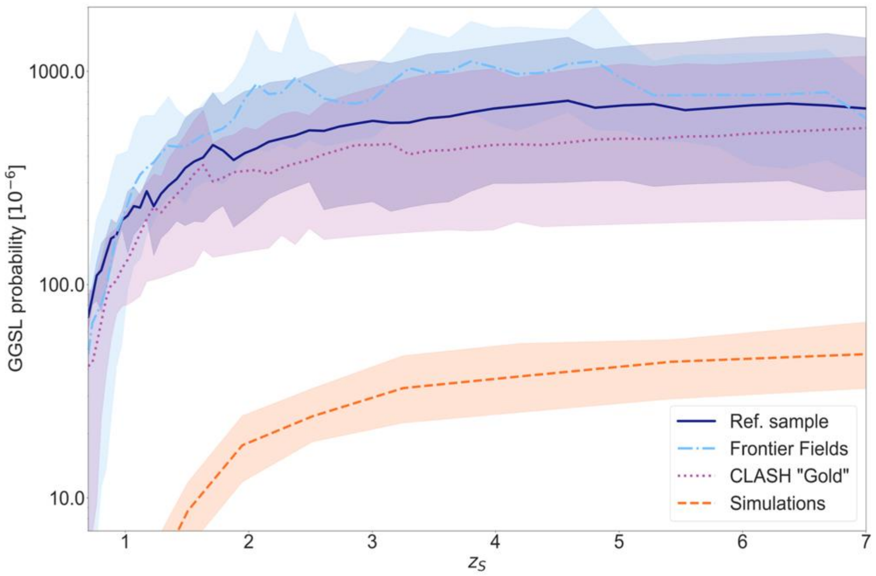

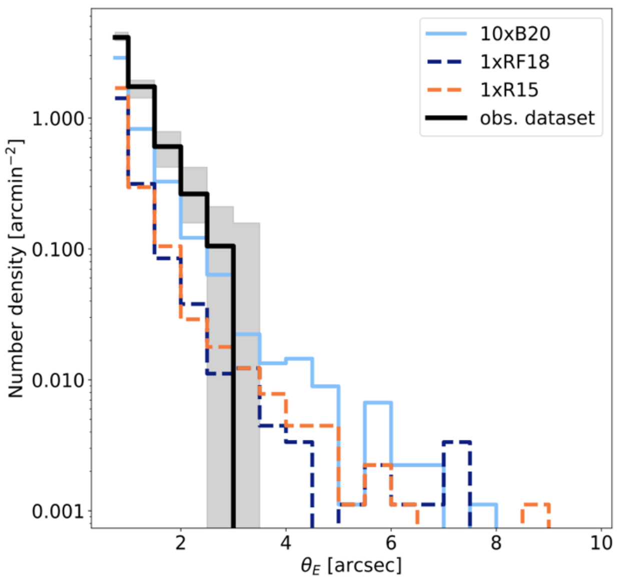

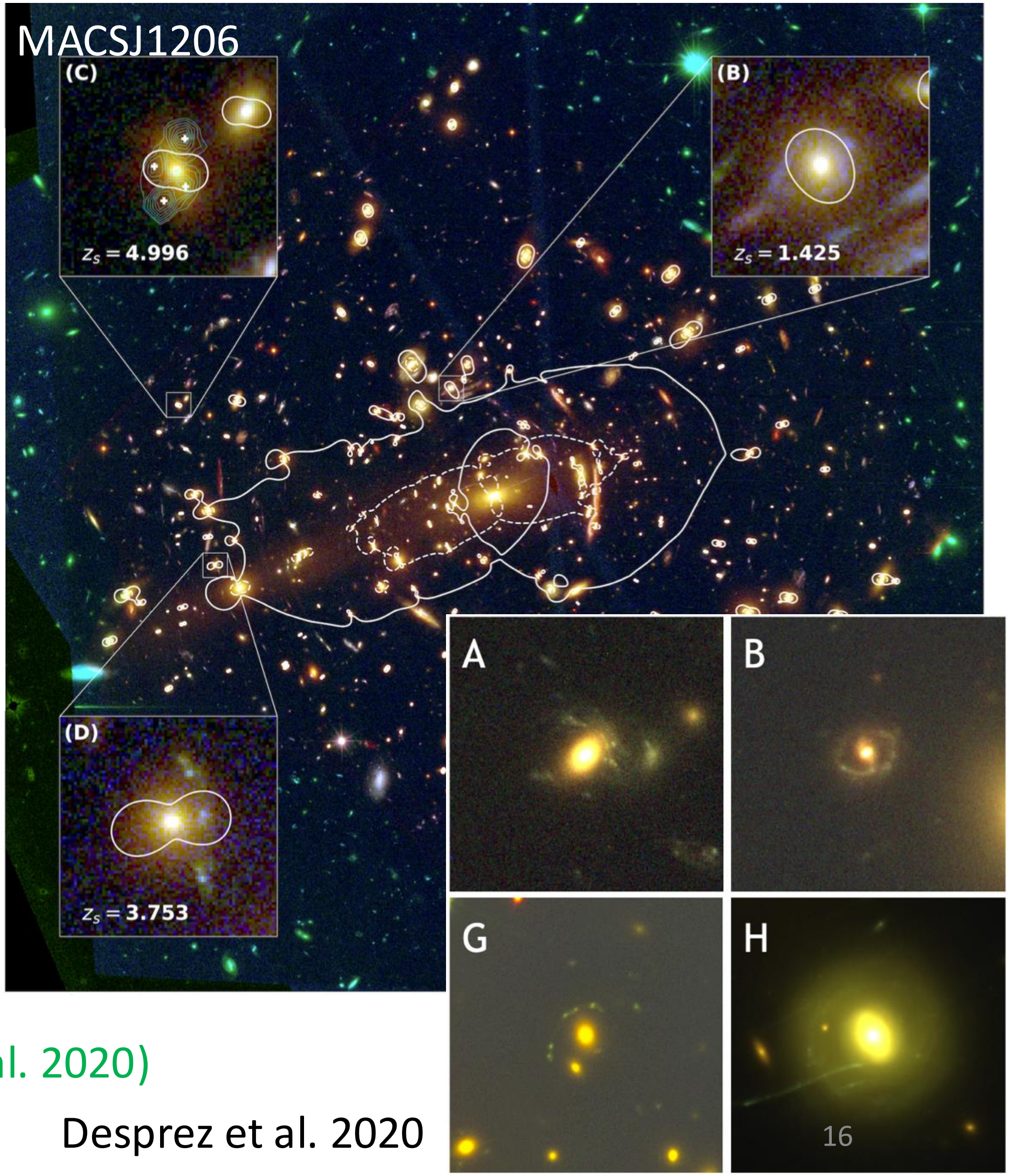

Compared to simulations (including baryons)

⇒ Observations present too many GGSL events

⇒ Substructures have smaller Einstein radius $\boldsymbol{\theta}_{\mathrm{E}}$

Proposed solutions

⇒ SIDM produces less arcs but they are more magnified (Vega-Ferrero et al. 2020)

⇒ FDM produces more arcs than CDM but not enough (Kawai et al. 2024)

Desprez et al. 2020

Selection effect?

- Strong lensing lenses are biased objects (Foex et al. 2014, Sonnenfeld et al. 2024)
  - SL lenses are trixial objects
  - Elongated halos along the line of sight

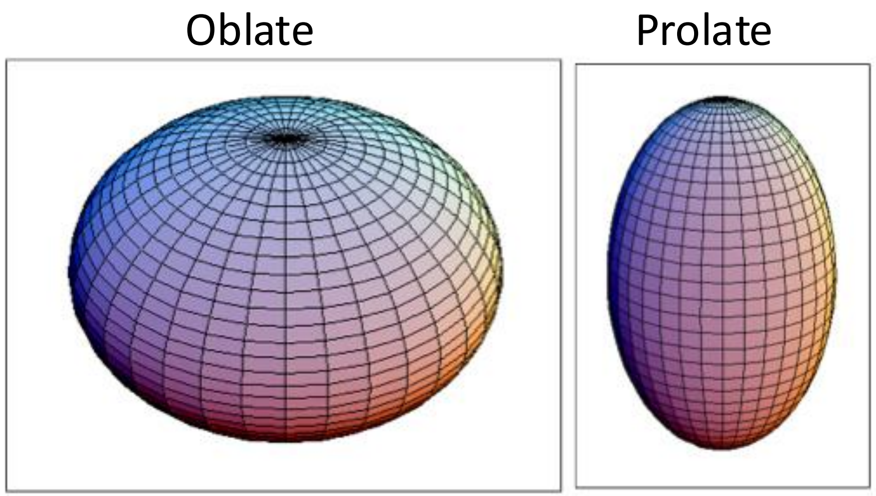

- Big efforts to characterize the selection function
  - Analytic predictions : including instrumental effects, e.g. Euclid, LSST, etc
  - Full hydro-simulations (e.g. Xu, Springel et al. 2017, Despali et al. 2021)
  - Spectroscopic observations : characterize redshift distribution of lenses and arcs (e.g. VLT-Xshooter program, PI: Jullo; 4MOST proposal PI: Collett; DESI secondary program Huang et al. in prep)

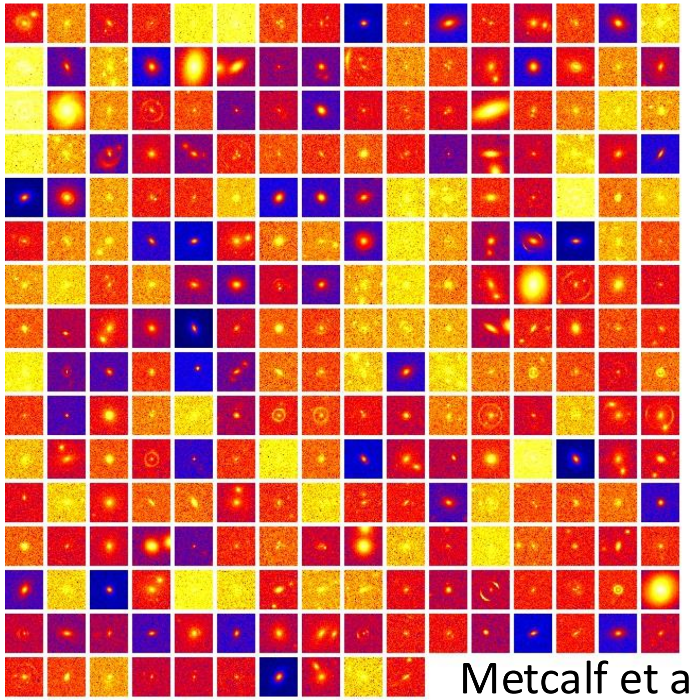

Metcalf et al. 2016

Einstein rings by galaxies

- Flux or position perturbation in Einstein rings reveals low mass subhalos (see also Chan et al. 2020 with axion part.)
- With optical/NIR observations in spectroscopy (~4h K-band/Keck, 3h NICMOS) => ~10^8 $M_\odot$/h
- Around 10^5 Einstein rings to be discovered with Euclid => good sample of « jackpot » candidates

Combined constraints Lya, lensing, MW satellites :

=> Lepton with asymmetries L6 > 10 and 7.1 keV sterile neutrinos are ruled out

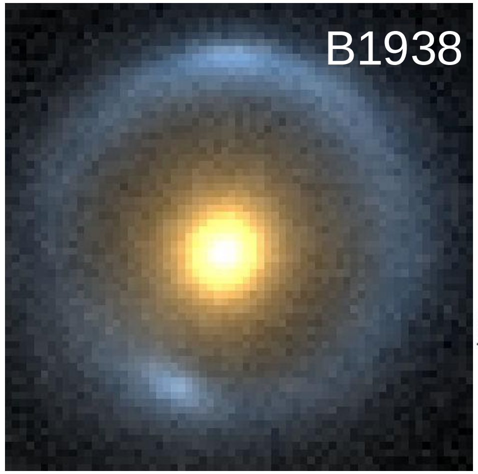

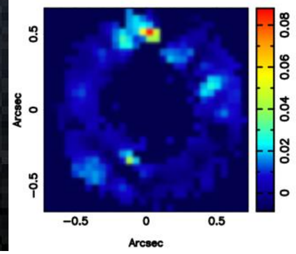

Vegetti et al. 2012

Constraints with 17 ER

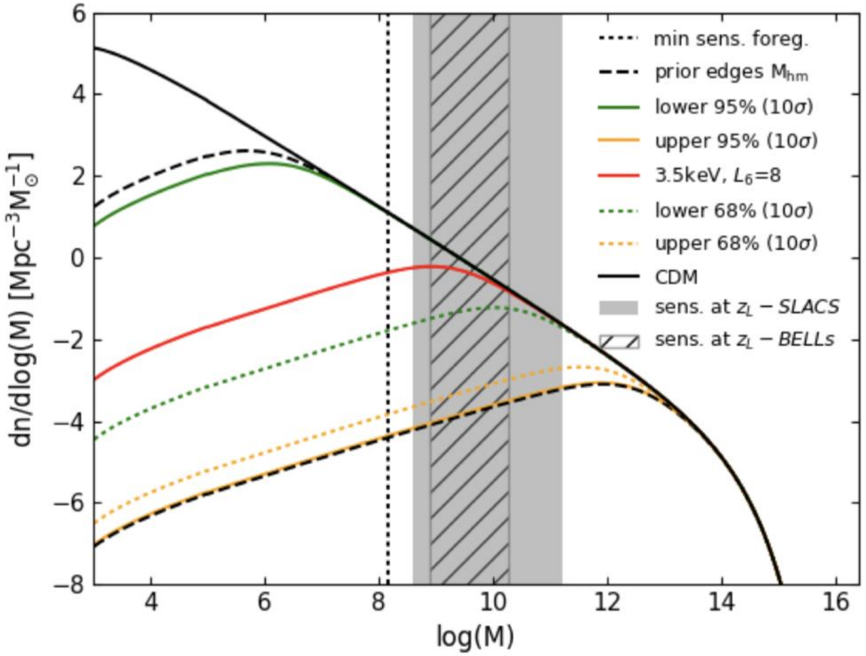

Ritondale et al. 2019

Quadruply imaged quasars : flux anomalies

- More small-scale substructures produce more frequent flux ratio anomalies
- Require long term monitoring of QSO flux variations
- Impact of Line of Sight structures (He, Li et al. 2021)
- Dependence on the simulation details (e.g. tidal destruction severity)

=> Move from standard modeling to summary statistics techniques to simplify the analyses

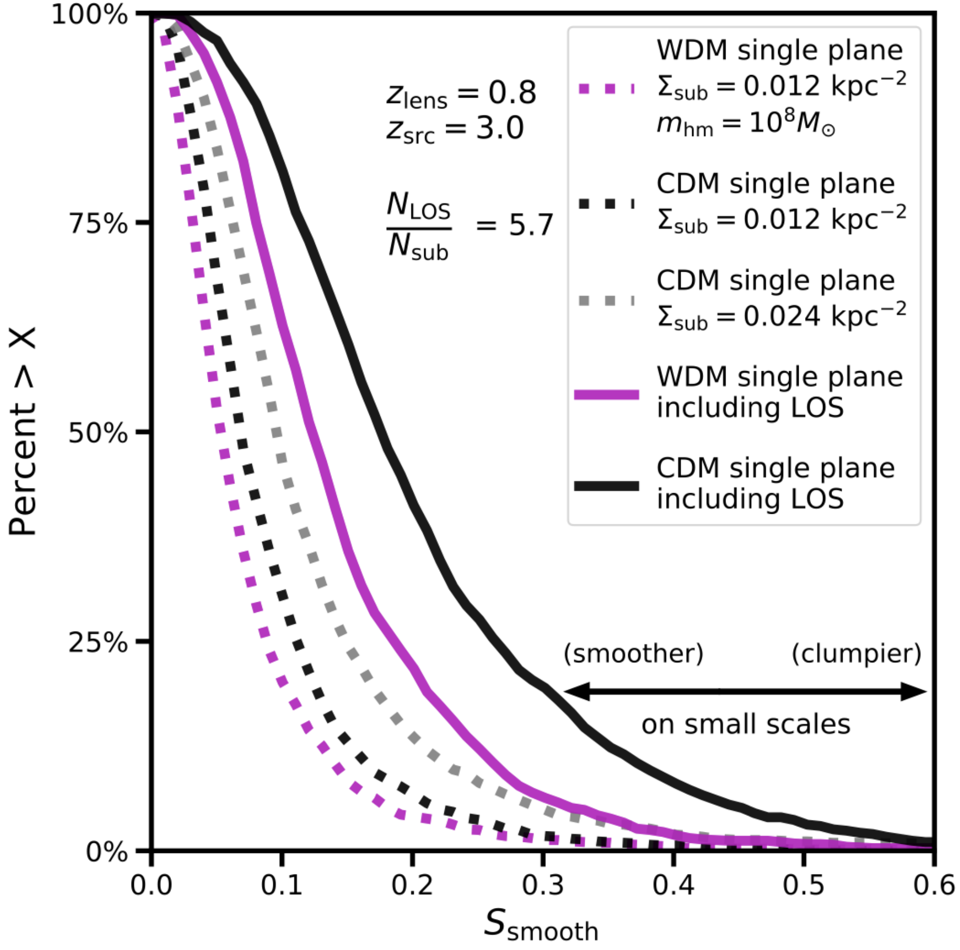

Gilman et al. 2021

Combined constraints: Lya, SL, MW sat.

Enzi et al. 2021

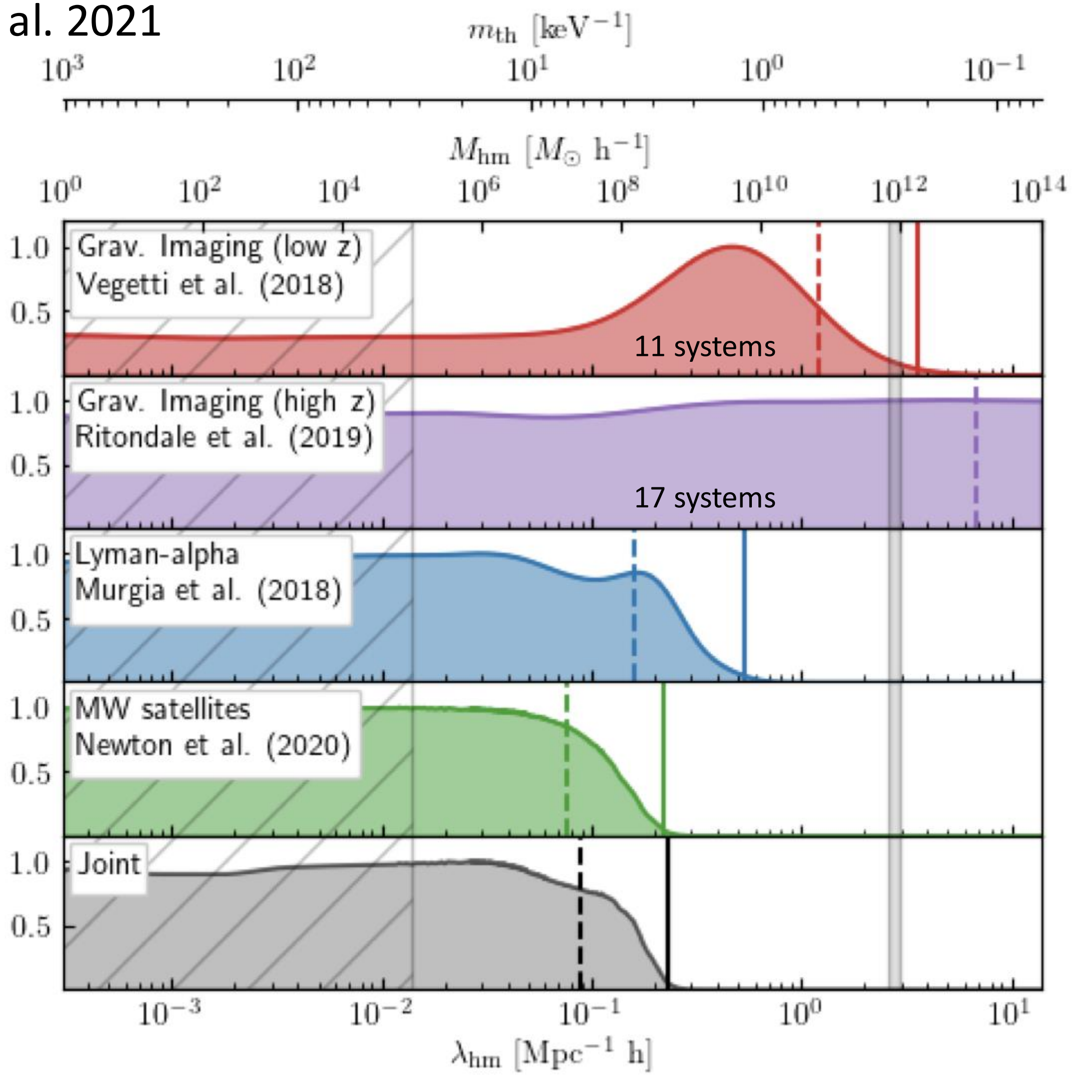

- VLBI + ELT will reach 0.2 to 5 mas resolution to probe halos 10^6 $M_\odot$ (Spingola et al. 2018 for VLBI)
- JWST will allow to maximize contribution from LOS haloes for High-z sources => tighter constraints
- Euclid & LSST will bring many candidates (~10^5)
- High-resolution, realistic hydro simulations will yield better dark matter models

=> For lepton asymmetries L6 > 10 , 7.1 keV sterile neutrinos are ruled out

Preparing the future: ELT-HARMONI simulations

- ELT-HARMONI expected first light ~2030
  - 42m telescope with Laser Guide Stars Adaptive Optics
  - IFU in NIR with 4mas spaxel resolution

- Simulated observations
  - Background galaxy at z = 2 with star formation clumps
  - Lens galaxy in 10^{13} $M_{\odot}$ halo
  - Perturbation 10^{8} $M_{\odot}$
  - Observational setup: Total exptime 5h, K grism, 30x60mas spaxels, LTAO, no moon, airmass 1.3
- Perturbation on the arc : 0.2±2 pixels => detection limit

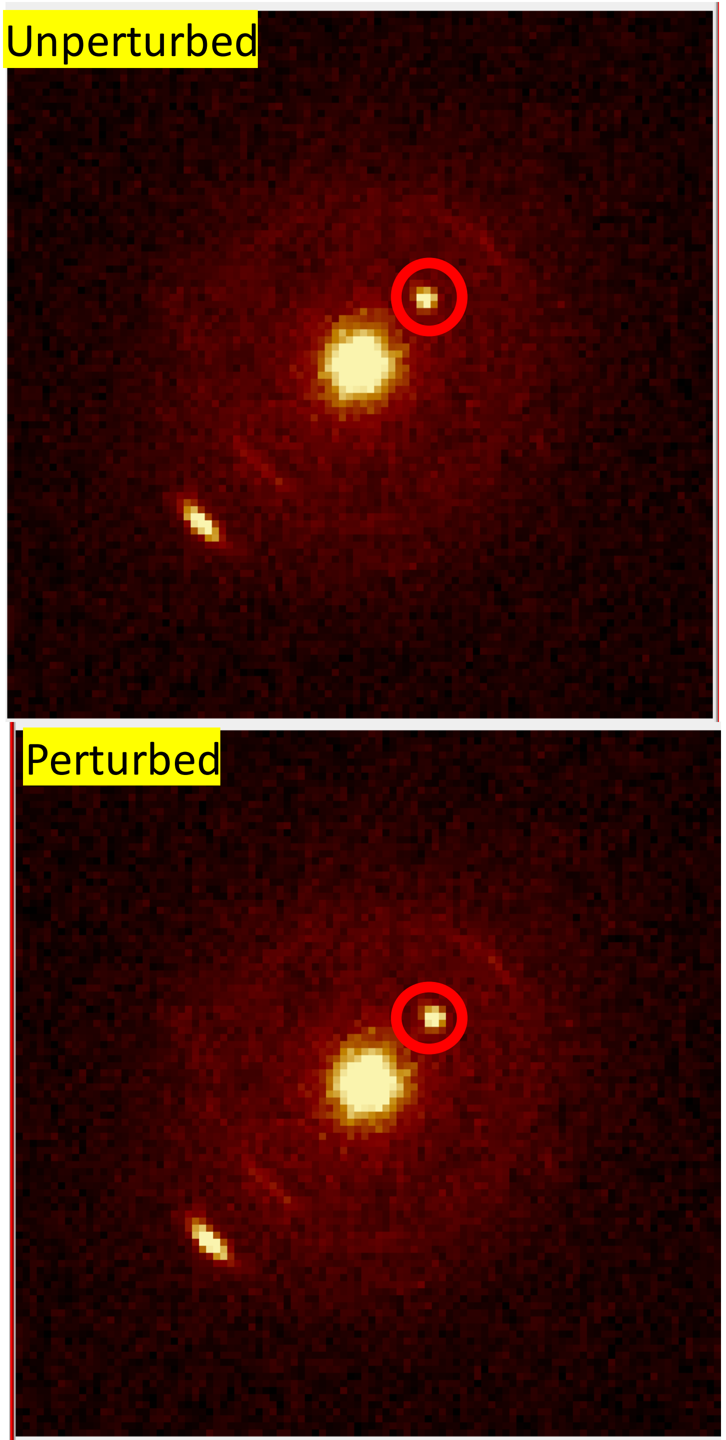

How to join effort?

Vegetti et al. 2012

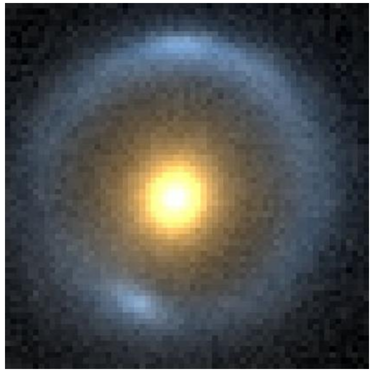

SL current constraints

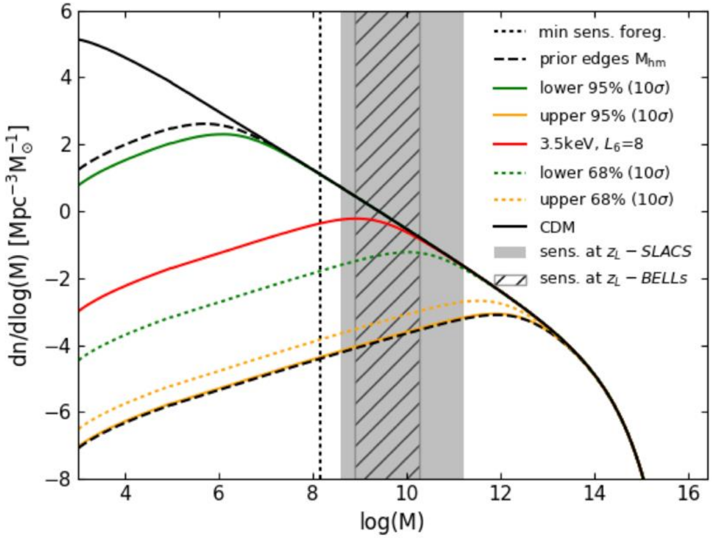

1) Gravitational lenses

=> WIMP & axion: galactic scale CDM behavior => unable to distinguish WIMP & axion?

2) Detection of DM particles

=> Sensitivity depends on the density model of the Galaxy and subhalos
=> use of simulations, observations (lensing, galaxy rotation curves, etc.)

In the 2 cases

- Use of hydrodynamical simulations

Simulation (Springel et al. 2008)

Much to gain by exchanging/joining efforts between communities 1) and 2), especially at the level of simulations

Milky Way modelling for direct detection

1. Hydrodynamical N-body (zoom-in) simulations including subhalos
2. Connecting cosmo simulations with astroparticles and dark matter detection
3. Phase space distribution beyond the Maxwellian distribution of the Standard Halo Model

Nezri et al. 2012
arXiv:1204.4121

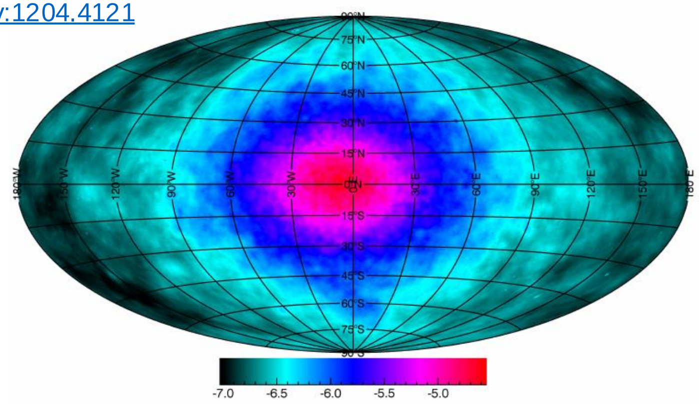

Petač et al. 2021
arXiv:2106.01314

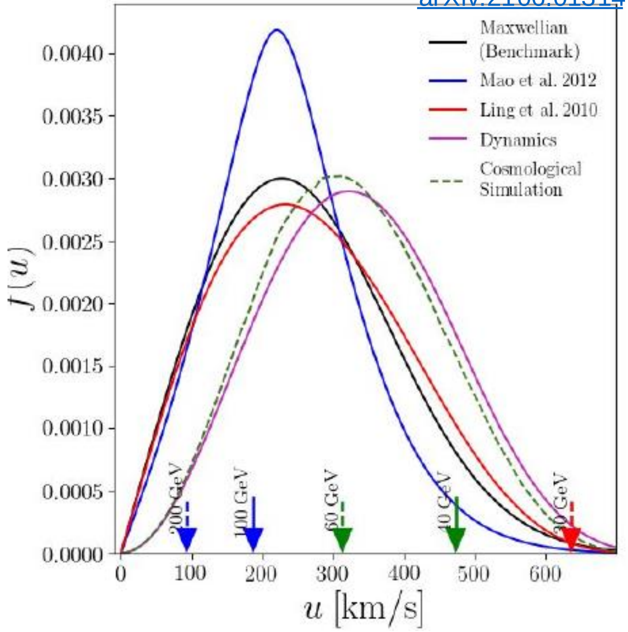

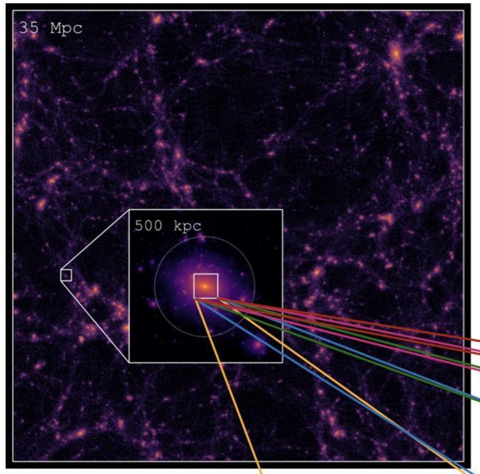

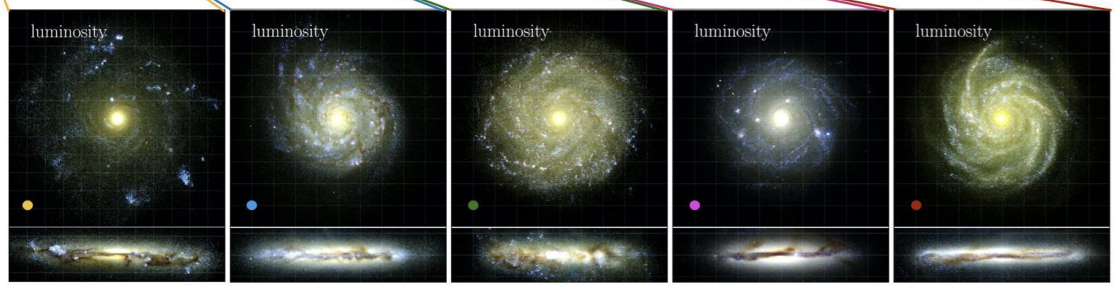

arXiv:1405.4318

Nuñez et al. 2022
arXiv:2004.06008

- Velocity distribution is more complex than analytical models => need simulations

=> Observations with gravitational lenses can constrain halo models and simulation

Dark Matter direct detection sensitivities

We assume a two-photon coupling to the axion (Ressell 1991, Bershady et al. 1991)

Two-photon coupling leads to monochromatic emission line

Gravitational lensing is used to determine the cluster density profile, and apply optimal weighting for emission line detection

VLT-VIMOS IFU observations image the core of the cluster

$$I_{\lambda_o} = 2.68 \times 10^{-18} \times \frac{m_{a,eV}^7 \xi^2 \Sigma_{12} \exp[-(\lambda_r - \lambda_a)^2 c^2/(2\lambda_a^2 \sigma^2)]}{000(1+z_{cl})^4 S^2(z_{cl})} \text{ cgs,}$$

$$\lambda_a = 24\,800 \text{ Å}/m_{a,eV} \quad (4)$$

=> Updated results with MUSE in dwarf spheroidal galaxies (Todarello 2024)

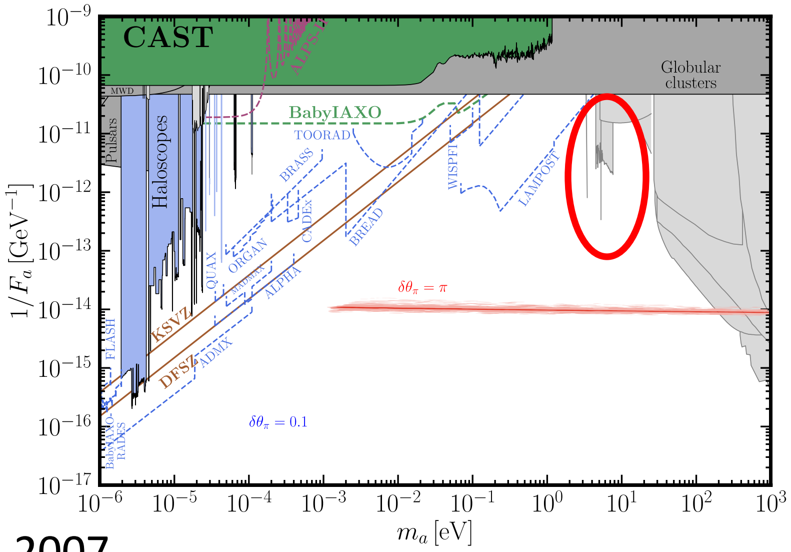

Grin et al. 2007

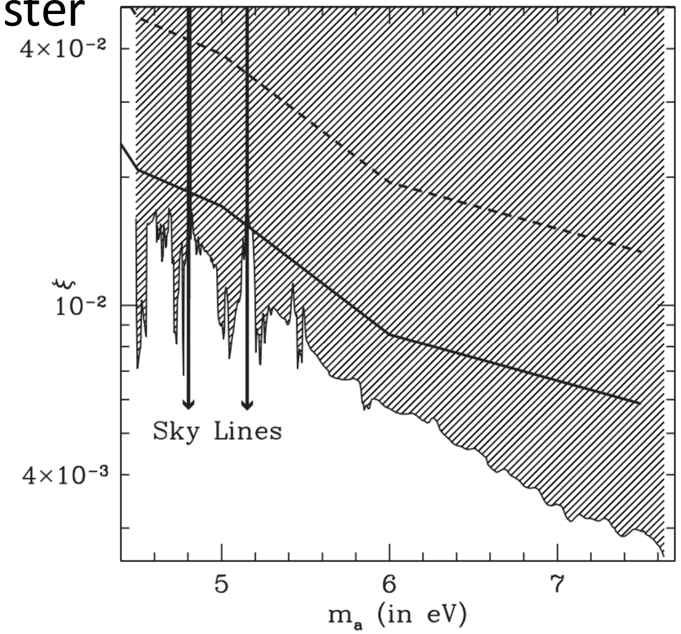

Scalar Field Dark Matter (SFDM) at small scales

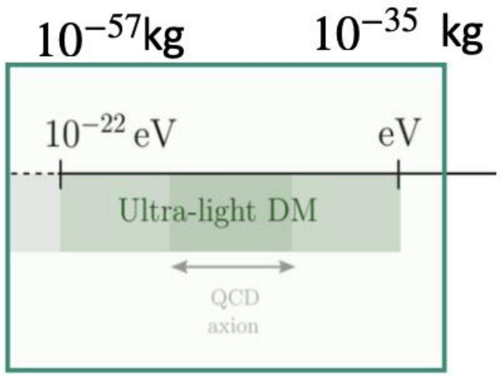

Because of its ultra-light mass → Large de Broglie wavelength, λ_{dB}~$1/mv$

- λ_{dB}~ pc — kpc
- Small scales: wavelike behaviour.
- **Solitons**: stable equilibrium configurations → **Flat density profile at the center of the halos.**

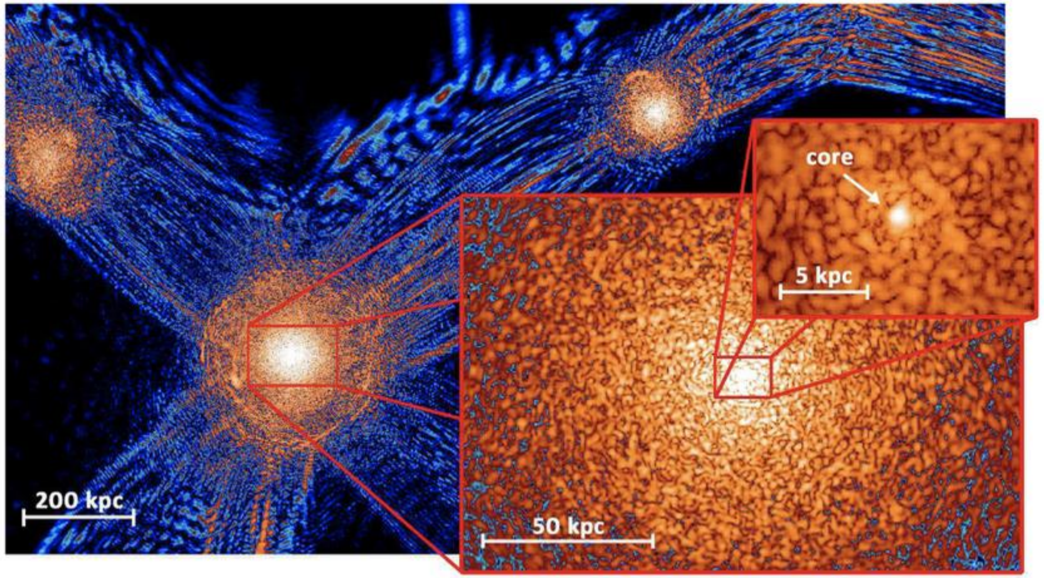

A slice of density field of ψDM simulation on various scales at z=0.1

Schive, Chiueh, and Broadhurst (2014)

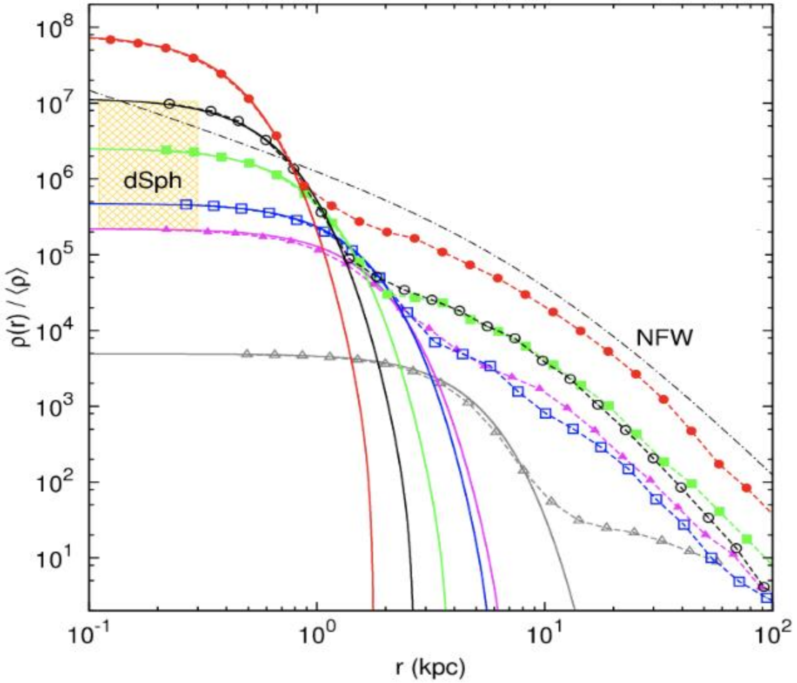

Radial density profiles of haloes formed in the ψDM model

=> See Talk by Raquel Galazo-Garcia

Study case: Halo $M \sim 10^{15} M_\odot$

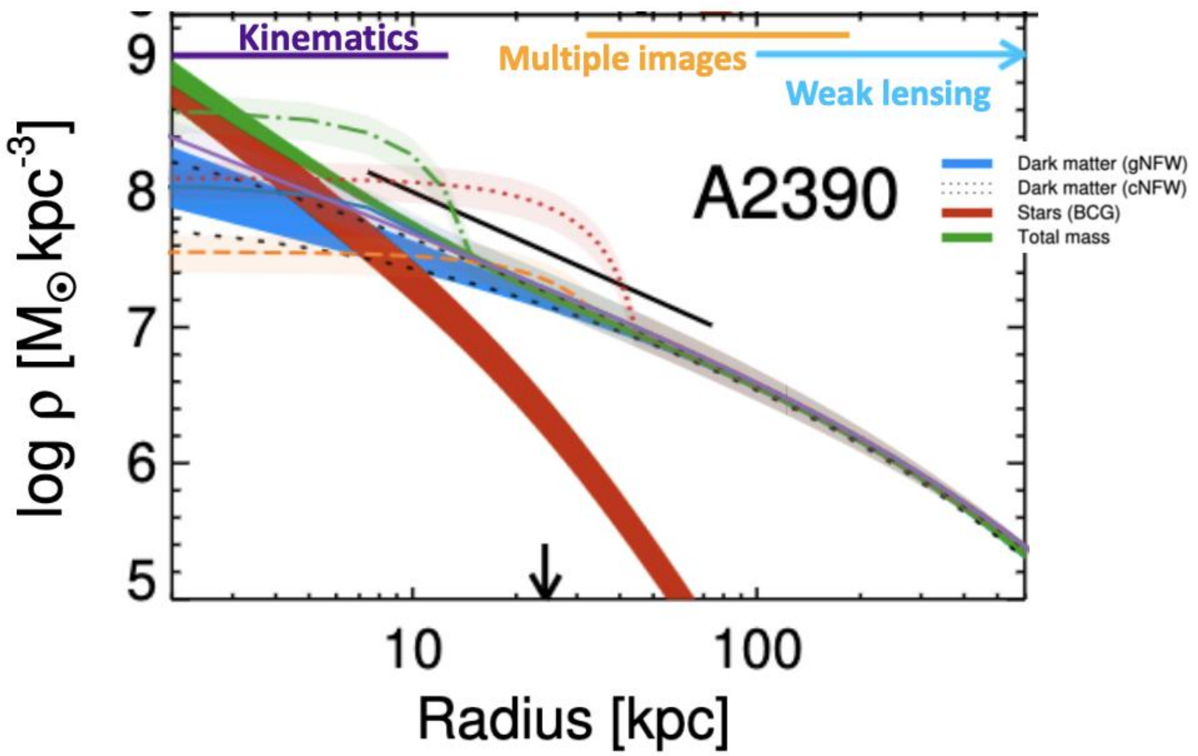

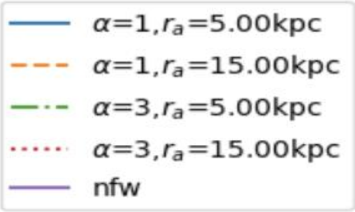

Halo $M = 2 \cdot 10^{15} M_\odot$						
α	r_a (kpc)	r_t (kpc)	ρ_c $(M_\odot/kpc^3)$	M_{sol} $(M_\odot)$	$f_{sol}(\%)$	$\Delta M_h\%$
1	5	10.90	$1.02 \cdot 10^8$	$3.31 \cdot 10^{11}$	0.016	$8.28 \cdot 10^{-8}$
1	15	32.06	$3.26 \cdot 10^7$	$2.75 \cdot 10^{12}$	0.137	$6.15 \cdot 10^{-8}$
3	5	14.50	$3.64 \cdot 10^8$	$1.75 \cdot 10^{12}$	0.087	0.058
3	15	43.36	$1.14 \cdot 10^8$	$1.48 \cdot 10^{13}$	0.74	0.49

Comparison with Andrew B. Newman, Tommaso Treu, Richard S. Ellis, and David J. Sand, 2013

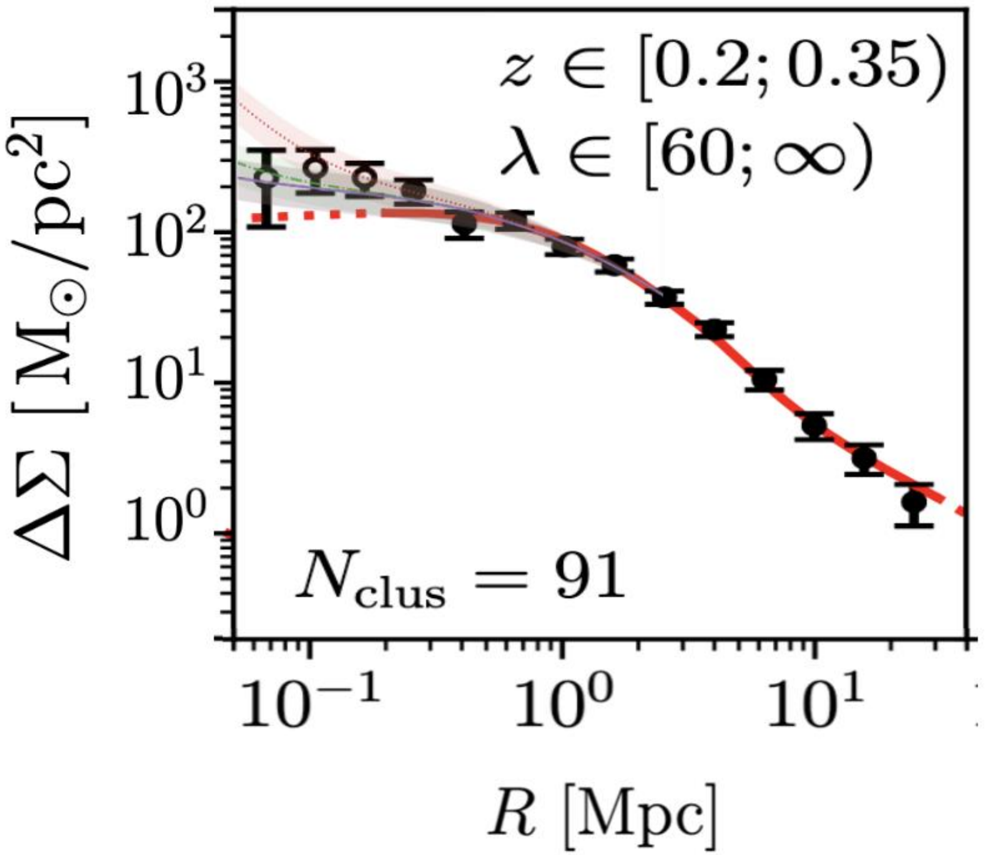

Comparison with Dark Energy Survey Year 1 Results: Weak Lensing Mass Calibration of redMaPPer Galaxy Clusters 2018

Credit: Raquel Galazo-Garcia

Another approach: FDM granules

In ψDM simulations (~Mpc size boxes, Schive et al. 2014), small halos have large granule size $l_\sigma \propto M^{-1/3}$
e.g. central soliton core r_c ~ 300 pc and mass ~ $10^{8.5}$ $M_\odot$, granules of mass 10^6 $M_\odot$

Model granule size: $l_\sigma = \hbar / m_a \, \sigma_v$
Variance of the granule density field: $\langle \delta\Sigma^2(r_\perp) \rangle = \sqrt{\pi} \langle l_\sigma \rangle \int dz \langle \rho_\psi(r) \rangle$

Observations with VLBI interferometer in radio (Powell et al. 2023)
=> undistinguishable from CDM at m_χ > 4.4 x 10^{-21} eV

Chan et al. 2020, Powell et al. 2023

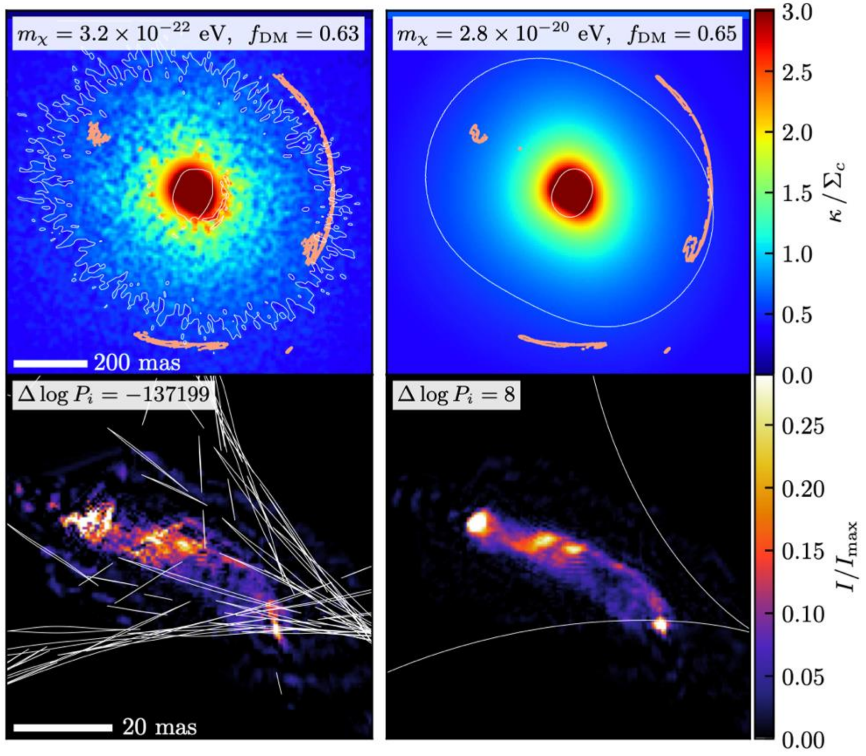

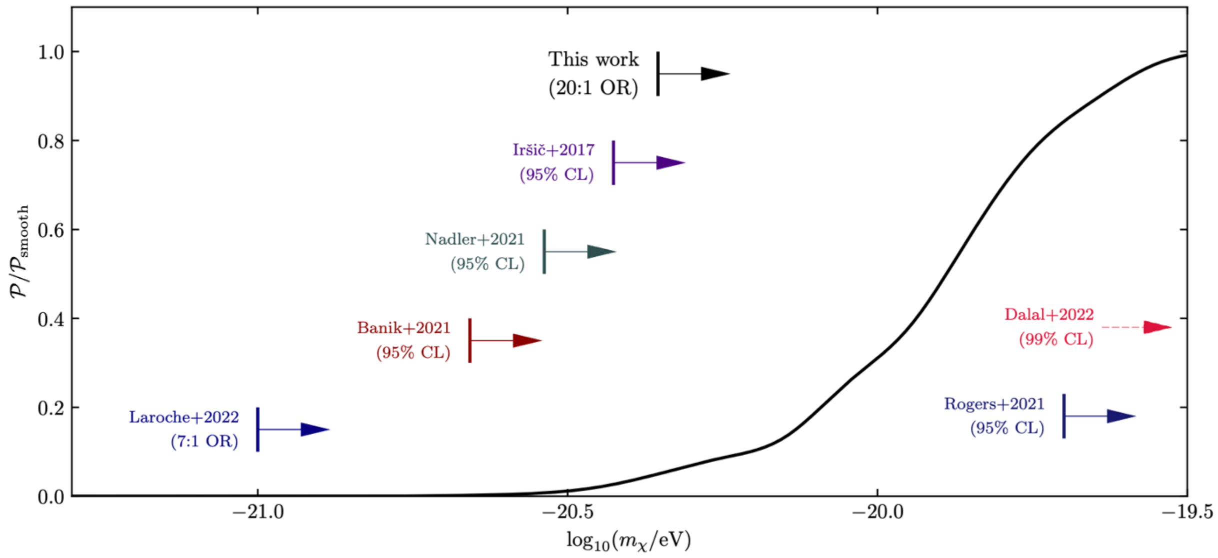

Take home messages

1. Combination of WL+SL+Kinematics is used to measure the slope γ of the dark matter density profile from galaxies to clusters
2. Uncertain stellar masses still impede firm conclusions on γ
3. Wide imaging surveys (eg. Euclid, LSST) will provide large samples of galaxies and clusters for stacking => selection function!
4. Future observations (ELT) will constrain the subhalo mass function
5. Selft Interacting axion model is promising and compatible with cluster constraints so far